Geoscientific
Model Development

Performance of the Adriatic Sea and Coast (AdriSC) climate component – a COAWST V3.3-based one-way coupled atmosphere–ocean modelling suite: ocean results

Petra Pranić[1], Cléa Denamiel[1,2], and Ivica Vilibić[1,2]

[1]Physical Oceanography Laboratory, Institute of Oceanography and Fisheries, Šetalište I. Meštrovića 63, 21000 Split, Croatia
[2]Division for Marine and Environmental Research, Ruđer Bošković Institute, Bijenička cesta 54, 10000 Zagreb, Croatia

Correspondence: Petra Pranić (pranic@izor.hr)

Abstract. In this study, the Adriatic Sea and Coast (AdriSC) kilometre-scale atmosphere–ocean climate model covering the Adriatic Sea and northern Ionian Sea is presented. The AdriSC ocean results of a 31-year-long (i.e. 1987–2017) climate simulation, derived with the Regional Ocean Modeling System (ROMS) 3 km and 1 km models, are evaluated with respect to a comprehensive collection of remote sensing and in situ observational data. In general, it is found that the AdriSC model is capable of reproducing the observed sea surface properties, daily temperatures and salinities, and the hourly ocean currents with good accuracy. In particular, the AdriSC ROMS 3 km model demonstrates skill in reproducing the main variabilities of the sea surface height and the sea surface temperature, despite a persistent negative bias within the Adriatic Sea. Furthermore, the AdriSC ROMS 1 km model is found to be more capable of reproducing the observed thermohaline and dynamical properties than the AdriSC ROMS 3 km model. For the temperature and salinity, better results are obtained in the deeper parts than in the shallow shelf and coastal parts, particularly for the surface layer of the Adriatic Sea. The AdriSC ROMS 1 km model is also found to perform well in reproducing the seasonal thermohaline properties of the water masses over the entire Adriatic–Ionian domain. The evaluation of the modelled ocean currents revealed better results at locations along the eastern coast and especially the northeastern shelf than in the middle eastern coastal area and the deepest part of the Adriatic Sea. Finally, the AdriSC climate component is found to be a more suitable modelling framework to study the dense water formation and long-term thermohaline circulation of the Adriatic–Ionian basin than the available Mediterranean regional climate models.

1 Introduction

Due to the temporal and spatial sparsity of in situ observations, the study of the dynamics and variability of the ocean processes mostly relies on constant developments and improvements of the available numerical modelling tools. Over the years, in the Adriatic Sea, significant progress has thus been made by the ocean modelling community to overcome the challenges posed by the complex geomorphology of the region (Fig. 1a and b): (1) an extremely complex coastline with over 1200 islands along the eastern coast, (2) bathymetries ranging from a shallow shelf (30 m on average) in the north to a very deep pit (up to approximately 1200 m) in the south, and (3) mountain ranges – Alps in the north, Apennines in the west, and Dinarides in the east – surrounding the semi-enclosed elongated Adriatic basin.

Historically, numerous studies have focused on the numerical modelling of the dense water formation and spreading in the Adriatic due to its vital role for many ocean processes such as the Adriatic–Ionian thermohaline circulation (Orlić et al., 2006; Vilibić et al., 2013), the Adriatic–Ionian Bimodal Oscillation System (hereafter referred to as BiOS; Gačić et al., 2010, 2014), and the biogeochemical properties of the ocean (Gačić et al., 2002; Krasakopoulou et al., 2005; Boldrin et al., 2009; Batistić et al., 2014). The initial numerical efforts in studying dense water formation in
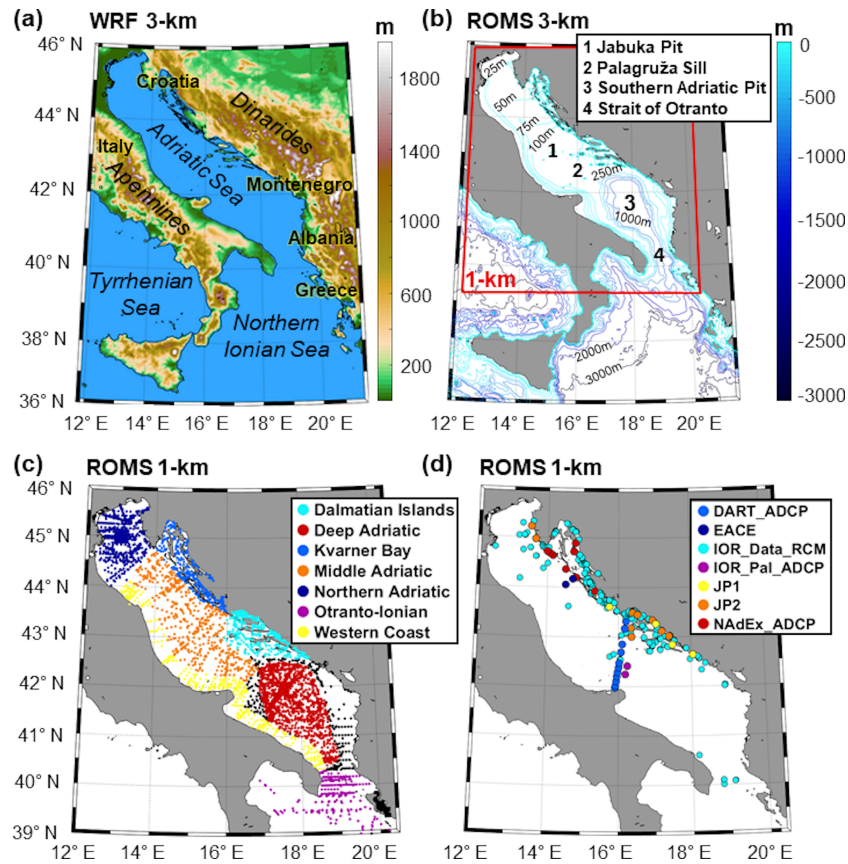
Figure 1. (a) AdriSC WRF 3 km domain and orography with geographical locations. **(b)** AdriSC ROMS 3 km and ROMS 1 km domains with bathymetry. The location of both **(c)** conductivity–temperature–depth (CTD) observations separated into seven subdomains and **(d)** acoustic Doppler current profiler (ADCP) or rotor current meter (RCM) measurements from seven different sources.

the Adriatic, with ocean model resolutions up to 3 km, were mainly focused on the North Adriatic Dense Water NAdDW) formation within the northern Adriatic shelf (Bergamasco et al., 1999; Beg-Paklar et al., 2001) and the Adriatic Deep Water (AdDW) formation within the southern Adriatic Pit and its interannual variability (Mantziafou and Lascaratos, 2004, 2008). At the time, the atmospheric fields used to force the ocean models were mostly climatological data (May, 1982; Artegiani et al., 1997) or the ECMWF (European Centre for Medium-Range Weather Forecasts) global datasets (e.g. ERA 40, ERA-I; Vested et al., 1998; Zavatarelli et al., 2002; Oddo and Guarnieri, 2011). However, many studies have demonstrated that the ECMWF reanalyses, due to their spatial homogeneity and coarse resolution, could not properly reproduce the extreme bora events driving the dense water formation in the northern Adriatic Sea. In particular, Cavaleri and Bertotti (1997) highlighted the fact that the underestimation of the bora wind speed could reach up to 50 %, which consequently led to a strong underestimation of NAdDW production rates (Vilibić and Supić, 2005). Therefore, in some studies, the ECMWF wind speeds have been increased by up to 20 % in order to improve the representation

of the ocean dynamics during bora events (e.g. Mantziafou and Lascaratos, 2004). More recently, the implementation by Janeković et al. (2014) of a modelling system based on the Regional Ocean Modeling System (ROMS; Shchepetkin and McWilliams, 2009) at 2 km of resolution forced by the operational atmospheric model ALADIN/HR (Aire Limitée Adaptation Dynamique développement InterNational; Tudor et al., 2013) has allowed for a better representation of the atmosphere–ocean dynamics during bora events in the northern Adriatic (Vilibić et al., 2016; Mihanović et al., 2018; Vilibić et al., 2018), which is also substantially influenced by the ocean feedback to the atmosphere (Pullen et al., 2006, 2007; Ličer et al., 2016).

In the last decade, other studies have also used kilometre-scale limited-area models to simulate ocean processes driven by extreme conditions in the Adriatic Sea, including, for example, extreme waves and storm surges, sea surface cooling, water column mixing, dense water formation, and long-term thermohaline circulation occurring during severe bora and sirocco windstorms (e.g. Cavaleri et al., 2010, 2018; Ricchi et al., 2016; Carniel et al., 2016; Denamiel et al., 2020a). However, aside from the atmospheric forcing, other sources

of errors have been documented to influence the quality of Adriatic numerical modelling such as the representation of the river discharges and the choice of the open boundary conditions. Concerning the problems associated with the river discharges, the use of old river climatologies (Raicich, 1994) and the lack of recent river load observations, in particular along the eastern Adriatic coast, resulted in large overestimation (multiplied by 5 at least) of the discharges in the northeastern Adriatic (Janeković et al., 2014). However, these old climatologies have been used in many recent Adriatic modelling studies (e.g. Zavatarelli and Pinardi, 2003; Oddo et al., 2005; Benetazzo et al., 2014), despite being proved to prevent dense water generation in the coastal eastern Adriatic area (Mihanović et al., 2013) and to decrease the ocean density for up to $0.5\,\mathrm{kg\,m^{-3}}$ in the primarily dense water formation sites in the northern Adriatic shelf (Vilibić et al., 2016). Concerning the propagation of errors from the open boundaries (particularly at the Strait of Otranto), they have mostly been documented as an underestimation of the salinity also linked to wrong freshwater forcing (Janeković et al., 2014). Other sources of errors, like improper parameterization of vertical mixing and diffusion, can also affect the performances of Adriatic models, and better ocean modelling solutions can be reached through a data assimilation procedure (Janeković et al., 2020). Notwithstanding the corrections of the above-mentioned sources of error, a common key conclusion of all the recent Adriatic studies was still the need for higher-resolution atmospheric models and longer-term simulations to capture the coastal ocean dynamics in the Adriatic Sea.

In terms of long-term climate modelling, the Adriatic Sea has, until now, dominantly been studied with regional climate models (RCMs) developed over the entire Mediterranean Sea within the Med-CORDEX initiative (e.g. Somot et al., 2006; Sevault et al., 2014). However, these RCMs have been shown to be incapable of properly reproducing the processes at the coastal scale mainly due to their relatively coarse horizontal resolution (of the order of 10 km), which is insufficient to resolve the complexity of the coastal morphologies of the Adriatic (McKiver et al., 2016; Dunić et al., 2019). In addition, some quasi-climate ocean studies were carried out to quantify interannual variability of the Adriatic dense water dynamics (e.g. Mantziafou and Lascaratos, 2004, 2008), while quantification of the sources for the Adriatic–Ionian decadal thermohaline variability required multi-decadal climate simulations of the eastern Mediterranean (Theocharis et al., 2014).

Therefore, to quantify the impacts of climate change in the Adriatic, it is crucial to obtain an adequate representation at climate scales of the atmosphere–ocean interactions during extreme events, which are, for example, driving the formation of dense water within the basin. Atmospheric RCMs generally fail to provide such a representation, especially in the northern Adriatic where they cannot be used to study the extreme bora dynamics (Denamiel et al., 2020b, 2021a). Ad-

ditionally, it has also been recently demonstrated that the latest higher-resolution ECMWF reanalysis dataset – the ERA5 product (Hersbach et al., 2018) – cannot be used as a reference for climate model evaluation or as a forcing for ocean models during bora events in the northern Adriatic as it also strongly underestimates the extreme bora speeds (Denamiel et al., 2021a). Consequently, in the recent study of Liu et al. (2021) – which investigated the BiOS variability using a regional ocean circulation model at 9 km resolution driven by the ERA-20C atmospheric forcing (Poli et al., 2016) with a 101-year-long simulation – the impact of bora events not properly represented by the atmospheric forcing was mimicked by artificially setting the 2 m air temperature and the dew point temperature over the entire Adriatic Sea to 0 °C in January, February, November, and December.

Following the findings of previous research, a need for higher-resolution atmospheric models – which are capable of reproducing the wind dynamics and air–sea interactions in the northern Adriatic – has been raised. Nevertheless, the development of high-resolution atmosphere–ocean models in areas of the Mediterranean, which are inadequately represented by regional climate models, is still not in the focus of the Med-CORDEX climate community, mainly because of their extremely high computational costs (Prein et al., 2015). The high-resolution atmosphere–ocean Adriatic Sea and Coast (AdriSC) climate model (up to 3 km in the atmosphere and 1 km in the ocean) was thus implemented, and a 31-year-long evaluation simulation was performed for the 1987–2017 period. In this work, the performance of the AdriSC ocean coastal model is evaluated, while the skill assessment of the AdriSC atmospheric kilometre-scale model is done in a separate study (Denamiel et al., 2021b). In general, a proper evaluation of a high-resolution climate model is not a trivial task and most often the biggest challenge turns out to be the availability, incompleteness, and scarcity of observational data, as well as the imperfections of the observing systems, which set further limits on the evaluation process (Horak et al., 2021). More specifically, the evaluation of ocean climate models is known to be particularly challenging due to the sparsity and inhomogeneity in time of ocean observations (Somot et al., 2018). Additionally, the absence of standardized gridded products in the Adriatic Sea renders the intercomparison of the skills of such ocean climate models extremely difficult. To overcome these challenges, significant effort has been made in this study to collect, from various sources and institutions, a large number of historical observational ocean data, especially long-term records and products with high temporal resolution and spatial coverage.

In the following section, the AdriSC climate component and the set-up of the AdriSC ocean model as well as the observations and methods used to perform the skill assessment of the model are presented first. Then, in Sect. 3, the main results of the study are presented and discussed in detail. They consist of three different kinds of evaluations: (1) sea surface (sea surface height and temperature) properties, (2) thermo-

haline properties (temperature and salinity), and (3) dynamical properties (current speed and direction). Lastly, the findings of this study are summarized in Sect. 4.

2 Model, data, and methods

2.1 AdriSC climate model

The Adriatic Sea and Coast (AdriSC; Denamiel et al., 2019) climate component is built around a modified version of the Coupled Ocean–Atmosphere–Wave–Sediment–Transport (COAWST V3.3) modelling system (Warner et al., 2010) in order to provide kilometre-scale hourly results for 31-year-long simulations as described in Denamiel et al. (2021b). In this study, the ocean results of the evaluation run for the 1987–2017 period – which can be easily accessed and retrieved via the web interface at https://vrtlac.izor.hr/ords/adrisc/interface_form (last access: 17 September 2021) (Ivanković et al., 2019; Denamiel et al., 2021b) – are presented in detail, while the set-up of the AdriSC climate model is summarized in Table 1. Hereafter, the Adriatic atmospheric processes are simulated with the Weather Research and Forecasting (WRF v3.9.1.1) model (Skamarock et al., 2005) for a 3 km grid covering the entire Adriatic and northern Ionian Sea (Fig. 1a). Concerning the ocean, the Regional Ocean Modeling System (ROMS svn 885; Shchepetkin and McWilliams, 2009) reproduces (1) the Adriatic–Ionian exchanges with a 3 km grid (266×361) identical to the atmospheric domain (Fig. 1a) and (2) the complex coastal Adriatic Sea dynamics with a one-way nested 1 km grid (676×730) receiving temperature, salinity, ocean currents, and sea surface elevation at its boundaries from the AdriSC ROMS 3 km model. Finally, the data exchanges between the WRF 3 km atmospheric grid and the ROMS 3 km and 1 km ocean grids are achieved with the Model Coupling Toolkit (MCT v2.6.0; Larson et al., 2005), and the remapping weights are computed with the Spherical Coordinate Remapping and Interpolation Package (SCRIP). Additionally, as no ROMS grid was set up to entirely cover the spatial domain of the WRF 15 km grid, the ROMS sea surface temperature (SST) is not prescribed to the WRF models in order to avoid the generation of discontinuities along the border between the two-way nested WRF 15 km and WRF 3 km atmospheric grids. Consequently, the only grid exchanges in the AdriSC modelling suite consist of the WRF 3 km model providing atmospheric fields (i.e. horizontal wind at 10 m, temperature at 2 m, relative humidity at 2 m, mean sea level pressure, downward shortwave radiation, longwave radiation, rain, and evaporation) to the ROMS 3 km and 1 km models, which increases the efficiency of the AdriSC model.

Ideally, a two-way coupling which imposes the SST of the ocean models on the atmospheric models should be used in climate studies. Indeed, it allows for better representation of the SST, which is known to impact local and regional precip-

Table 1. Summary of the AdriSC climate component ocean model main features for the evaluation run.

Ocean model	ROMS
Number of domains	2
Horizontal resolution	3 km $\;\mid\;$ 1 km
Vertical resolution	35
Time step	150 s $\;\mid\;$ 50 s
Fields exchanged from ROMS 3 km to ROMS 1 km	temperature, salinity, ocean currents, sea surface elevation
Atmospheric forcing (frequency)	WRF 3 km (30 min)
Initial and boundary conditions (frequency)	MEDSEA (daily)
31-year period	1987–2017
Frequency of outputs	Hourly

itation (Mejia et al., 2018; Yang et al., 2019; Johnson et al., 2020). In the AdriSC modelling suite the two-way coupling would require the use of an additional ROMS 9 km grid covering the WRF 15 km domain. However, due to limited numerical resources and the slowness of the AdriSC modelling suite, such a set-up could not be envisioned in this study. As a consequence, within the AdriSC modelling suite, the WRF models do not benefit from the more accurate simulation of the SST done with the ROMS models. This is also true for future scenario runs which only add climatological changes (e.g. increase in SST up to 3.5 °C in summer) to the SST forcing used in the evaluation run following the pseudo-global warming (PGW) method originally developed for the atmosphere (Schär et al., 1996) and extended to the ocean by Denamiel et al. (2020a).

As described in Denamiel et al. (2021b), the COAWST model is compiled with the Intel 17.0.3.053 compiler, the PNetCDF 1.8.0 library, and the MPI library (mpich 7.5.3) on the European Centre for Medium-Range Forecasts (ECMWF) high-performance computing facility (HPCF). Furthermore, the ecFlow workflow package used by all ECMWF operational suites is set up to automatically and efficiently run the AdriSC long-term simulations in a controlled environment. Regarding the workload, the AdriSC climate model optimally runs on 260 CPUs with both the WRF and ROMS grids decomposed in 10×13 tiles and without hyper-threading.

For a complete presentation of the AdriSC climate component, a detailed description of the set-up of both atmospheric and oceanic models is necessary. Since the evaluation of the AdriSC climate model is done separately for the atmosphere (Denamiel et al., 2021b) and the ocean, only the set-up of the

AdriSC ROMS 3 km and the one-way nested AdriSC ROMS 1 km models is described below.

First, a digital terrain model (DTM), including (1) coastline data generated by the Institute of Oceanography and Fisheries, (2) offshore bathymetry from ETOPO1 (Amante and Eakins, 2009), and (3) nearshore bathymetry from navigation charts CM93 201, provides high-resolution bathymetry data for both AdriSC ROMS grids. Moreover, the bathymetry (with the minimum depth of 2 m) is smoothed with the application of a linear programming (LP) method (Dutour Sikirić et al., 2009) to the ROMS 3 km and 1 km grids. In this way the roughness factors are minimized while keeping the DTM bathymetric features. Also, the horizontal pressure gradient errors generated by the use of terrain-following coordinates with steep bathymetric gradients are reduced. In the actual configuration of the AdriSC ROMS climate models, 35 vertical layers – transformed ($V_{\text{transform}} = 2$) and stretched ($V_{\text{stretching}} = 4$) following Shchepetkin and McWilliams (2009) – are used with increased resolution at the surface ($\theta_s = 6$) and bottom ($\theta_b = 2$) as well as a thickness of 50 m ($h_c = 50$).

Second, regarding the external forcing of the AdriSC ROMS 3 km model, the initial conditions and boundary forcing – including sea surface height, barotropic and baroclinic currents, and baroclinic temperature and salinity – are provided daily by the Mediterranean Forecasting System (MFS) MEDSEA v4.1 re-analysis (resolution of $1/16° \times 1/16°$; Pinardi et al., 2003) distributed by the Copernicus Marine Environment Monitoring Service (CMEMS). It should be noted that the SST used in the WRF models is also provided by the MEDSEA re-analysis as fully described in Denamiel et al. (2021b). The tidal forcing consists of eight tidal constituents (M2, S2, N2, K2, K1, O1, P1, Q1) extracted from the Mediterranean Sea and Black Sea (2011) $1/30°$ regional solution of the OSU Tidal Inversion Software (OTIS; Egbert et al., 1994; Egbert and Erofeeva, 2002). The tidal constituents used were previously found to adequately reproduce the tidal dynamics in the Adriatic Sea (Cushman-Roisin and Naimie, 2002; Janeković and Kuzmić, 2005). Concerning the river forcing, 54 river flows in total (only 49 for the 1 km grid) are imposed over at least six grid points each (and 18 grid points for the Po river delta), with river mouths located along the coastline of the Italian peninsula, Sicily, Croatia, Slovenia, Albania, Montenegro, and Greece. The monthly climatology of the river flow is acquired from the RivDis database (Vörösmarty et al., 1996) and studies from Pano and Abdyli (2002), Malačič and Petelin (2009), Pano et al. (2010), Janeković et al. (2014), and Ljubenkov (2015), whereas the river flow interannual variability is obtained from Ludwig et al. (2009). Additionally, the river flows are linearly distributed between the first 20 sigma vertical levels – i.e. the discharge is multiplied by weights ranging from 20/210 at the surface, to 19/210 at the first sigma level below the surface, to zero at the 20th sigma level below the surface.

Third, on the one hand, the high optical water clarity in shallow parts of the Adriatic such as the eastern Adriatic Sea creates a warming sea surface temperature (SST) trend linked to the absorption of the shortwave radiation reaching the seafloor, while, on the other hand, the low optical water clarity along the Italian coast due the muddy waters of the Po river plume tends to produce opposite trends. A dQ/dSST procedure, which is described in detail in the study of Denamiel et al. (2019), is thus used to solve this problem by minimizing the corrections of the heat fluxes produced by WRF while making sure that no artificial SST trends are generated in the shallow parts of the ROMS grids. In brief, this method imposes a heat flux correction through the calculation of the kinematic surface net heat flux sensitivity to the SST of reference. Consequently, the 9 km SST forcing from the MEDSEA v4.1 re-analysis is also used as a reference for the calculation of the dQ/dSST procedure with the ROMS model.

It should be noted that the use of the dQ/dSST procedure should not be seen as a permanent solution for climate studies in the Adriatic Sea. Indeed, the SST of reference used in future climate scenario runs is based either on other climate model predictions, which are by nature uncertain, or on approximations using climatological changes. Consequently, long-term research on the fine tuning and parametrization of the solar radiation penetration using, for example, ocean colour, turbidity, or even sediment transport modelling is thus a prerequisite for a better representation of the coupled atmosphere–ocean dynamics in the Adriatic Sea.

Fourth, the AdriSC evaluation run was initialized on 1 November 1986 in order to have a short 2-month spin-up period allowing the ocean models to reach a steady state. Indeed, short experiments have shown that rapid equilibrium is reached within the AdriSC ocean models due to (1) the use, before 1 January 1987, of monthly (instead of daily) MEDSEA v4.1 re-analysis products, which have a relatively fine resolution (about 9 km) and assimilate all available data in the Mediterranean Sea, and (2) the relatively small size of the ROMS ocean domains. Ideally, several long-term simulations should have been run with different spin-up periods in order to better quantify the impact of the initial conditions on the long-term ocean model results. However, due to numerical resource limitations, such systematic tests have not been carried out with the AdriSC climate model.

Finally, concerning the configuration of the physical options for the ROMS models, the MEDSEA barotropic velocities, surface elevations, and baroclinic fields at the open boundaries are imposed with the Flather (Flather, 1976), Chapman (Chapman, 1985), and Orlanski (Orlanski, 1976) conditions. Additionally, the baroclinic structure is relaxed – with a minimum folding time of 3 d – towards the fields provided by the MEDSEA ocean climatology (Marchesiello et al., 2001). The relaxation occurs in two different nudging areas: (1) a 10-grid-point-wide zone along the open boundaries and (2) a zone covering the bathymetry deeper than 2000 m

but only for the temperature and salinity in order to minimize the numerical diapycnal mixing. A sponge area of 10 grid points (identical to the first nudging area) also ensures that the horizontal viscosities are smoothly interpolated from values 4 times bigger at the open boundaries than inside the domain. Last, the tracer advection is provided with the Multidimensional Positive Definite Advection Transport Algorithm (MPDATA; Smolarkiewicz and Grabowski, 1990), while the horizontal momentum advection uses a fourth-order cantered scheme and the turbulence closure scheme follows the GLS gen framework (Umlauf and Burchard, 2003).

2.2 Skill assessment

2.2.1 Observations

In this study, the AdriSC ocean model (ROMS 3 km and one-way nested ROMS 1 km) performances are assessed for five different variables (sea surface height, temperature, salinity, ocean current speed and direction) by comparison to a comprehensive collection of observational data retrieved for the 1987–2017 period from in situ measurements and remote sensing gridded products.

The first dataset used in this study is the Sea Surface Height Anomalies (SSHA) gap-free remote sensing (L4) product, SEA_SURFACE_HEIGHT_ALT_GRIDS_L4_2SATS_5DAY_6THDEG_V_JPL1812 (Zlotnicki et al., 2019; hereafter referred to as JPL MEASURES). It has been produced at the Jet Propulsion Laboratory (JPL) of the Physical Oceanography Distributed Active Archive Center (PODAAC) on a 1/6° grid every 5 d since October 1992. The final gridded product, obtained by a kriging method, is a combination of SSHA data derived from TOPEX/Poseidon, Jason-1, Jason-2, and Jason-3 as reference data as well as ERS-1, ERS-2, Envisat, SARAL-AltiKa, and CRyosat-2, depending on the date.

Second, two different sea surface temperature (SST) gap-free remote sensing (L4) products were chosen for this evaluation. They were extracted from the datasets provided by the Group for High-Resolution Sea Surface Temperature (GHRSST), which offers a framework for SST data sharing and processing. The first product, AVHRR_OI-NCEI-L4-GLOB-v2.0 (National Centers for Environmental Information, 2016; hereafter referred to as AVHRR), has been produced daily on a 0.25° grid at the National Oceanographic and Atmospheric Administration (NOAA) National Centers for Environmental Information (NCEI) since September 1981. It uses optimal interpolation (OI) by interpolating and extrapolating SST observations from the Advanced Very High-Resolution Radiometer (AVHRR) and in situ platforms (i.e. ships and buoys), resulting in a smoothed complete field. The main advantage of AVHRR is thus that it covers the entire 1987–2017 period of the AdriSC evaluation run. However, its resolution is rather coarse and is likely to be insufficient to properly describe the coastal areas of the Adri-

atic basin. Consequently, a high-resolution second product is also used in this study for a shorter period. The MUR-JPL-L4-GLOB-v4.1 (JPL MUR MEaSUREs Project, 2015; hereafter referred to as JPL MUR) has indeed been produced daily on a global 0.01° grid at the JPL of the PODAAC since June 2002. It uses wavelets as basis functions in an OI approach. The Multiscale Ultrahigh Resolution (MUR) analysis is based upon nighttime GHRSST SST observations from several instruments including the National Aeronautics and Space Administration (NASA) Advanced Microwave Scanning Radiometer-EOS (AMSR-E), the JAXA Advanced Microwave Scanning Radiometer 2 on GCOM-W1, the Moderate Resolution Imaging Spectroradiometers (MODIS) on the NASA Aqua and Terra platforms, the US Navy microwave WindSat radiometer, the AVHRR on several NOAA satellites, and in situ SST observations from the NOAA iQuam project.

The third dataset consists of a comprehensive collection of temperature and salinity in situ conductivity–temperature–depth (CTD) observations with diverse temporal and spatial coverage (Fig. 1b). This dataset combines 17 different experiments and/or scientific cruises: (1) Argo floats – ARGO (https://argo.ucsd.edu, last access: 20 September 2021), (2) ASCOP project Phase 2, Istituto Nazionale di Oceanografia e di Geofisica Sperimentale (OGS), (3) Corfu System Project – CSP01 cruise (https://isramar.ocean.org.il/PERSEUS_Data, last access: 20 September 2021), (4) Dynamics of the Adriatic in Real Time – DART_CTD (Martin et al., 2009; Burrage at al., 2009), (5) CTD observations, Institute of Oceanography and Fisheries (IOR) – IOR_Data_CTD, (6) Palagruža transect long-term observations – IOR_Pal_CTD, (7) Mediterranean Data Archaeology and Rescue project – MEDATLAS (http://www.ifremer.fr/medar/cdrom_database.htm, last access: 20 September 2021), (8) Northern Adriatic Experiment CTD observations – NAdEx_CTD (Vilibić et al., 2018), (9) Otranto Gap Experiment, SACLANT Undersea Research Centre – OTRANTO, (10) PALMAS, OGS, (11) PCO, Consiglio Nazionale delle Ricerche (CNR), Istituto di Biologia del Mare, Venice, (12) Physical Oceanography of the Eastern Mediterranean project, Hellenic National Oceanographic Data Centre (HCMR/HNODC) – POEM, (13) Programma di RIcerca e Sperimentazione del Mare Adriatico Phase 2 (chemical stations) hosted at OGS – PR2_UR, (14) Programma di RIcerca e Sperimentazione del Mare Adriatico Phase 1 hosted at OGS – PRISMA, (15) PRV, CNR, Istituto di Biologia del Mare, Venice, (16) Northern Adriatic long-term observations, Ruđer Bošković institute – RB_NAd (Vilibić et al., 2019), and (17) SIRIAD cruise hosted at OGS – SIRIAD_15. This large dataset includes over 7000 locations in total and covers the Adriatic Sea almost entirely and partially the northern Ionian Sea. Data sampling frequency varies largely depending on the locations and the observations, while the maximum depth of the measurements ranges between 40 and 2140 m. All CTD observa-

tions had already been independently quality checked except IOR_DATA_CTD, which was quality controlled in this study to automatically and visually remove outliers, values with steep gradients, and vertical instabilities using standard procedures described in the SeaDataNet manual (https://www.seadatanet.org/Standards/Data-Quality-Control, last access: 20 September 2021).

Finally, the last dataset is a collection of ocean current speed and direction combining acoustic Doppler current profiler (ADCP) and rotor current meter (RCM) in situ observations with diverse temporal coverage (Fig. 1c). This dataset combines seven different experiments and/or scientific cruises: (1) Dynamics of the Adriatic in Real Time – DART_ADCP (Martin et al., 2009; Burrage at al., 2009), (2) East Adriatic Coastal Experiment – EACE (http://www.izor.hr/eace/eace_g.htm, last access: 20 September 2021), (3) historical RCM observations – IOR_Data_RCM, (4) Palagruža transect ADCP observations following the winter of 2012 – IOR_Pal_ADCP, (5) Jadranski project Phase 1 ADCP observations – JP1, (6) Jadranski project Phase 2 ADCP observations – JP2, and (7) Northern Adriatic Experiment ADCP observations – NAdEx_ADCP (Vilibić et al., 2018). All the observations had already been independently quality checked except for IOR_Data_RCM, which received an additional quality control performed to automatically and visually remove obvious outliers, spurious data, and long strings of constant values. A full list of the data collected to perform the AdriSC ROMS 3 km and one-way nested 1 km model evaluations during the 1987–2017 period is presented in Table 2. The table includes, for each of the four datasets (i.e. SSHA, SST, CTD, and ADCP/RCM), the name of the corresponding observations (i.e. remote sensing products as well as CTD and ADCP/RCM experiments and/or scientific cruises), the time period, the number of locations, the number of records, and the maximum measured depth.

2.2.2 Methods

Once the evaluation run is completed, the extraction of the AdriSC ROMS 3 km and the one-way nested AdriSC ROMS 1 km model hourly and daily results is achieved in two different ways. A bilinear interpolation to the coarser coordinates of the JPL MEASURES, AVHRR, and JPL MUR gridded products with the Earth System Modelling Framework (ESMF) software is performed for the comparison with satellite observations. For the comparison with the in situ observational datasets, a near-neighbour method at points in time and space matching the coordinates of the CTD, RCM, and ADCP stations is used before linear interpolation to the vertical structure of the measurements following the depth. Moreover, in order to obtain more robust statistics for the chosen geophysical quantities which are likely to be heavy-tailed due to extreme conditions, the use of median and median absolute deviation (MAD) is preferred to the mean and standard deviation recommended for normal distributions. Finally, the performance of the AdriSC ocean models is evaluated separately for each type of observational dataset (i.e. SSHA and SST remote sensing gridded products, CTD observations, and ADCP/RCM measurements).

Due to the relatively coarse temporal and spatial resolutions of the satellite observations, only the evaluation of the AdriSC ROMS 3 km model is performed against the selected sea level and sea surface temperature remote sensing products (i.e. SSHA from JPL MEASURES and SST from AVHRR and JPL MUR). For the sea level analysis, empirical orthogonal functions (EOFs) are used to compare, in space and time, the most important variability patterns in the Adriatic Sea and northern Ionian Sea. Indeed, Gačić et al. (2011) have demonstrated that the BiOS – consisting of the decadal switch from cyclonic to anti-cyclonic of the circulation in the northern Ionian Sea and greatly impacting the thermohaline circulation of the Adriatic Sea – is well described with the decadal change of sign of one of the main components of the EOF derived from SSHA products. The EOFs (also known as principal component analysis or eigen analysis) presented in this study are obtained via a covariance matrix and are normalized (i.e. the sum of squares for each EOF pattern equals 1). The time series of the amplitudes (also known as principal components or expansion coefficients) associated with each eigenvalue in the EOF are derived via the dot product of the data and the EOF spatial patterns, and the mean is subtracted from the value of each component time series. Consequently, EOFs performed on SSHA from remote sensing products and sea surface height (hereafter referred to as SSH) results from the AdriSC ROMS 3 km model can be directly compared despite the different mean sea level references used to derive SSHA and SSH. For the SST analysis, the bias or difference between model results and observations is calculated at each point in time and space of the AVHRR and JPL MUR datasets. The biases are then analysed in space with statistical quantities such as the median and the 1st, 25th, 75th, and 99th percentiles.

The skill assessment of the AdriSC ROMS 3 km and 1 km models against in situ temperature and salinity CTD data is divided into three main analyses. First, a basic assessment of the model performances is achieved with (1) Taylor diagrams (Taylor, 2001) using multiple statistical parameters, (2) quantile–quantile (Q–Q) plots comparing the distributions of the observed and modelled temperature and salinity, and (3) scatter diagrams that are unique for the AdriSC ROMS 1 km model, which is further used in the study as having a more precise matching of the nearest grid points with the CTD locations. The second analysis looks in more detail at the spatial distributions of the median and MAD of the biases between the AdriSC ROMS 1 km model and the CTD observations depending on the depth (i.e. for four different depth ranges: 0–50, 50–200, 200–500, and 500–2000 m). Finally, a climatological analysis of the AdriSC ROMS 1 km results is performed for seven different subdomains: western coast, northern Adriatic, middle Adriatic, Kvarner Bay, deep

Table 2. Name and period of the observations, number (no.) of locations and records, and maximum measured depth for the four datasets – i.e. (1) sea surface height anomalies (SSHAs), (2) sea surface temperatures (SSTs), (3) conductivity–temperature–depth (CTD) observations, and (4) acoustic Doppler current profiler (ADCP) or rotor current meter (RCM) measurements – used to evaluate the AdriSC ROMS 3 km and 1 km models over the 1987–2017 period.

Dataset	Observations	Period	No. locations	No. records (10^3)	Max. depth (m)
SSHA	JPL MEASURES	1992–2017	2065	3808	surface
SST	AVHRR	1987–2017	966	10 938	surface
	JPL MUR	2002–2017	46 777	266 348	surface
CTD	ARGO	2012–2017	2182	569	1503
	ASCOP	1990–1991	96	4	39
	CSP01	1991	108	5	64
	DART_CTD	2005–2006	502	64	1202
	IOR_Data_CTD	1987–2017	3043	419	1214
	IOR_Pal_CTD	2012	5	4	170
	MEDATLAS	1987–1990	254	63	2143
	NAdEx_CTD	2014–2015	19	4.5	93
	OTRANTO	1994–1995	332	231	1259
	PALMAS	1994	103	14	1154
	PCO	1987–1989	162	6	52
	POEM	1991–1992	85	44	1191
	PR2_UR	1996–1998	111	0.6	62
	PRISMA	1995–1996	538	236	1208
	PRV	1987–1988	283	1	38
	RB_NAd	1987–2017	6	9	40
	SIRIAD_15	2015	64	26	1199
	All data	1987–2017	7781	1700	2143
ADCP/RCM	DART_ADCP	2005–2006	11	2482	164
	EACE	2002–2003	2	282	68
	IOR_Data_RCM	1987–2004	321	268	930
	IOR_Pal_ADCP	2012	2	313	129
	JP1	2007–2009	4	430	82
	JP2	2013–2014	10	1784	79
	NAdEx_ADCP	2014–2015	8	940	83
	All data	1987–2015	358	9034	930

Adriatic, Dalmatian Islands, and Otranto–Ionian (Fig. 1c). For each subdomain, the following results are presented: (1) monthly climatology of the median (and MAD as upper and lower bounds) of the modelled and observed temperature and salinity – this analysis is done without taking the same depth range for each month due to the vertical scarcity of the measurements, (2) seasonal variations of the vertical profiles of median temperature and salinity biases interpolated to standard oceanographic depths selected appropriately for each subdomain – seasons are defined as January, February, and March (JFM) for winter, August, May, and June (AMJ) for spring, July, August, and September (JAS) for summer, and October, November, and December (OND) for autumn, and (3) seasonal variations of temperature–salinity (T–S) diagrams of observations and model results.

Lastly, the evaluation of the AdriSC ROMS 3 km and 1 km models against in situ ocean current speed and direction of the ADCP and RCM measurements is divided into two main analyses. First, a basic assessment of the model performances is achieved with (1) Taylor diagrams, (2) Q–Q plots comparing the distributions of the observed and modelled current speed and direction, and (3) scatter diagrams that are unique for the AdriSC ROMS 1 km model, which is further used for the other analyses. Second, a climatological analysis of the AdriSC ROMS 1 km results is performed for the seven different datasets (Fig. 1c) collected from experiments and/or scientific cruises described in Sect. 2.2.1. For each dataset, the following results are presented: (1) monthly climatology of the median (and MAD as upper and lower bounds) of the modelled and observed current speed and direction – this analysis is done without taking the same depth range for each month due to the vertical sparsity of the measurements, (2) seasonal variations of the vertical profiles of the modelled and observed median current speed interpolated to standard

oceanographic depths selected appropriately for each dataset – seasons are defined the same as for the CTD analysis, and (3) seasonal variations of the modelled and observed current direction presented in the form of polar histograms (i.e. rose plots) showing the current direction distributions.

3 Results and discussion

3.1 Modelled sea surface properties

3.1.1 Evaluation

First, the three main normalized spatial EOF components (Fig. 2) and associated amplitude time series (Fig. 3), derived from the JPL_MEASURES SSHA gridded product and the AdriSC ROMS 3 km SSH results, are analysed and compared.

Overall, it can clearly be seen that, for both the Adriatic Sea and northern Ionian Sea (Fig. 2), the first EOF component (EOF1) represents the seasonal variability of both AdriSC ROMS 3 km and JPL_MEASURES results, with spatial signal and amplitudes slightly stronger in the model (i.e. 81.2 % of the total signal with amplitudes varying ±8.0; Fig. 3) than in the observations (i.e. 74.5 % of the total signal with amplitudes ranging ±6.0; Fig. 3). Additionally, the correlation coefficient between the time variations of the observed and modelled EOF1 is only 0.65, associated with a normalized standard deviation of 1.19. The two remaining EOF components are switched in the model compared to the observations (Figs. 2 and 3). In other words, the second ROMS 3 km EOF component (EOF2 representing 6.2 % of the total signal) corresponds to the third SSHA EOF component (EOF3 representing 3.0 % of the signal) and vice versa. In addition, in the observations, the EOF2 component represents the decadal variability, while the EOF3 component shows the interannual variability of the SSHA signal (Fig. 3). The comparison between modelled spatial EOF2 and observed spatial EOF3 (Fig. 2) reveals that, for the interannual variability, the AdriSC ROMS 3 km results do not reproduce the observed eddies in the northern Ionian Sea and present different spatial patterns in the northeastern Adriatic. Further, the interannual variability signal is generally stronger in the ROMS 3 km model (varying mostly ±2.0; Fig. 3) than in the SSHA observations (ranging mostly ±1.0; Fig. 3). Consequently, as both seasonal and interannual signals are stronger in the AdriSC ROMS 3 km results than in the JPL_MEASURES observations, the decadal variability and hence the so-called BiOS signal in the northern Ionian Sea (pattern clearly identified with strongly negative EOFs values; Fig. 2) are weaker in the model (2.1 % of the total signal with amplitudes varying ±1.5; Fig. 3) than in the measurements (5.9 % of the total signal with amplitudes ranging ±2.0; Fig. 3). The differences between observations and modelling of the BiOS-driven signal can also be ob-
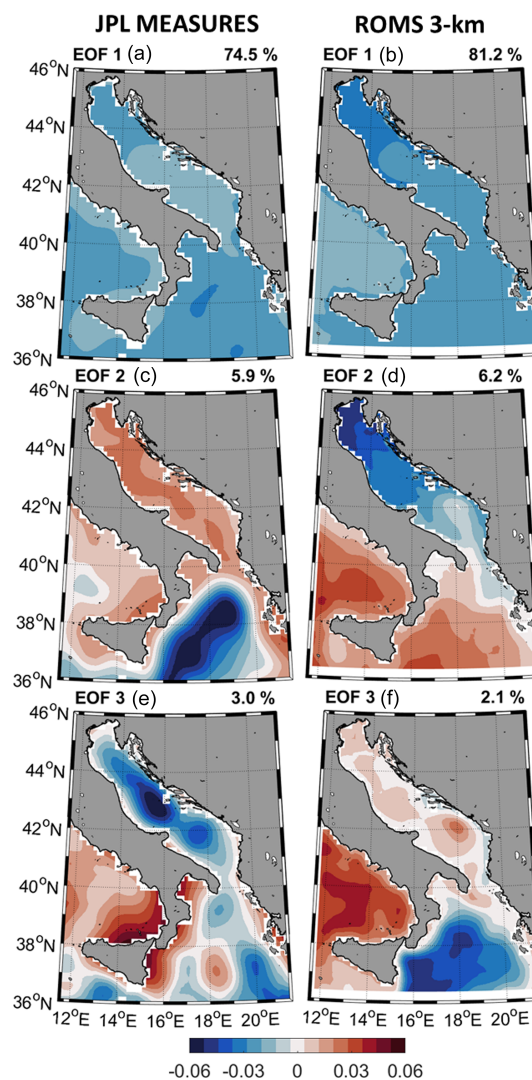

Figure 2. Three main normalized spatial EOF components derived during the 1993–2017 period from the SSHA from the JPL MEASURES gridded product (**a, c, e**) and the SSH results of the AdriSC ROMS 3 km model (**b, d, f**).

served during the 2012–2014 period after an intense dense water formation in 2012 (Mihanović et al., 2013), which had the capacity to reverse the circulation in the northern Ionian Sea (Gačić et al., 2014). Here, the modelled EOF3 reaches a substantially negative value in 2012 and particularly in 2013, while the observations (EOF2) only present a slight decrease in amplitude which mostly stays positive during these 2 years. As such, this may indicate a larger capacity of the dense waters to change the BiOS-driven patterns during these extremely severe years compared to other BiOS-driven amplitude reversals (e.g. 1997, 2005, and 2009), which are of a similar amplitude ratio in the ROMS 3 km model and the observations. Further, it may be hypothesized that the limited capability of the AdriSC ROMS 3 km model to reproduce the intensity of the BiOS signal is linked to the insufficient spa-
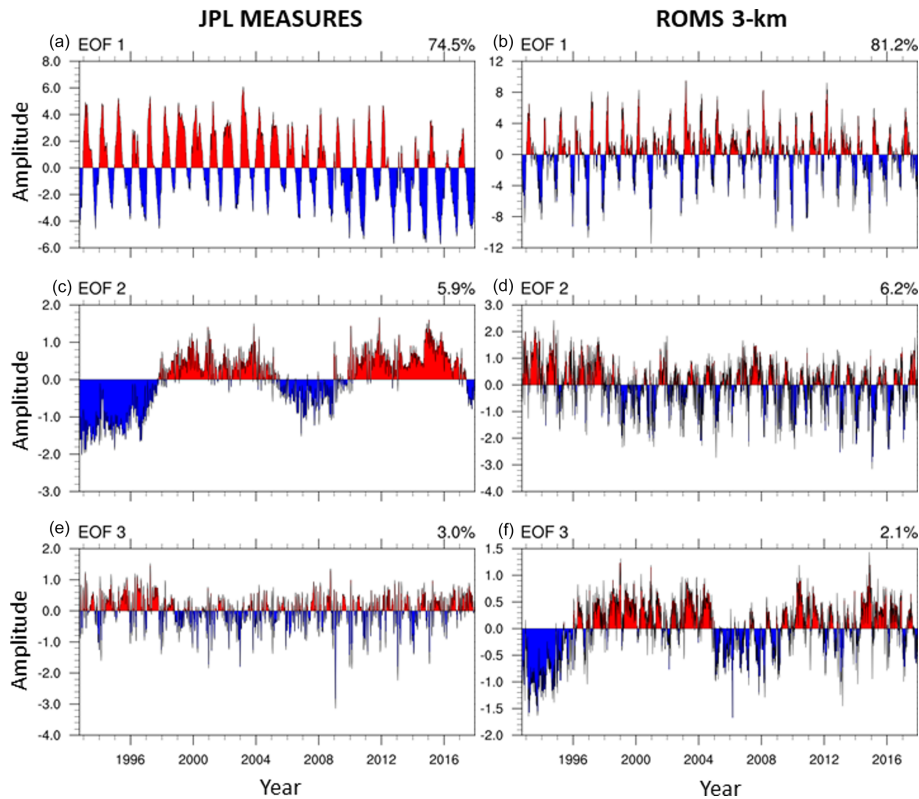
Figure 3. Time series of the amplitudes associated with the three main normalized spatial EOF components derived during the 1993–2017 period from the SSHA from the JPL MEASURES gridded product **(a, c, e)** and the SSH results of the AdriSC ROMS 3 km model **(b, d, f)**.

tial extension of the ROMS 3 km domain to the south, where the boundary conditions thus have too much influence on the obtained results. Finally, despite these limitations, it should also be noted that the time variations of the three main EOFs (Fig. 3) are overall well synchronized between the model and the observations.

The AdriSC ROMS 3 km sea surface temperature results are further compared to two different remote sensing products – i.e. AVHRR SST (Fig. 4) and JPL_MUR SST (Fig. 5) – with spatial maps of both the median of the gridded observations and the median as well as the 1st, 25th, 75th, and 99th percentiles of the biases between the AdriSC ROMS 3 km results and the observations.

The spatial variations of the AVHRR median observations (Fig. 4) show that the lowest temperatures are present in the northern and western parts of the Adriatic Sea, reaching around 17.0 °C on average. The middle and southeastern parts of the Adriatic have surface temperatures ranging from 17.5 to 19.0 °C. In the northern Ionian Sea median temperatures are higher, ranging from 18.0 to 19.8 °C. Regarding the evaluation, the AdriSC ROMS 3 km model underestimates the SST in the northern Adriatic, particularly along the plume of the Po river by down to −0.8 °C, while in the rest of the Adriatic biases are lower and range from −0.2 to 0.2 °C. In the Ionian Sea, the model tends to overestimate the SST by

up to 0.6 °C along the western coast and by 0.1 °C on average along the eastern coast. In terms of the extreme underestimations, the biases reach down to −2.0 °C in the northern Adriatic, −0.7 °C in the rest of the Adriatic, and −0.5 °C in the Ionian Sea for the 25th percentile as well as −4.0 °C in the northern Adriatic, −3.0 °C in the rest of the Adriatic, and −2.0 °C in the Ionian Sea for the 1st percentile. Small negative biases down to −0.5 °C are still present in the northern Adriatic for the 75th percentile, with positive biases up to 0.3 °C for the rest of the Adriatic and up to 1 °C in the Ionian Sea. For the 99th percentile, the whole domain presents positive biases around 1.5 °C in the Adriatic and 2 °C in the Ionian Sea. It should be noted that, in some coastal parts of the domain, the observed dark blue patches are artefacts resulting from different representations of the coastline between the AdriSC ROMS 3 km model and the AVHRR remote sensing product.

The other SST dataset analysed in this study (JPL_MUR SST) has a shorter temporal span (i.e. only starts in June 2002) but a higher spatial resolution (i.e. 0.01° instead of 0.25°) and thus a more accurate representation of the coastline than AVHRR. The median of the JPL_MUR_SST dataset (Fig. 5) shows that the lowest temperatures are present in the northern and northeastern Adriatic, reaching around 17.0 °C on average. The middle and western parts of
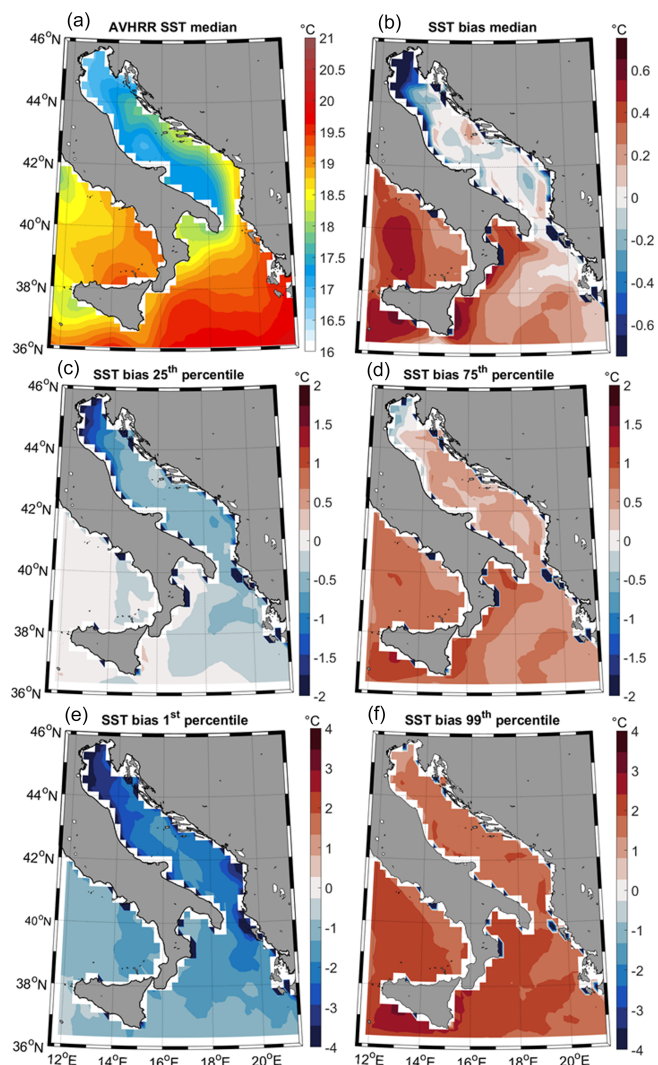
Figure 4. Median of the AVHRR daily sea surface temperature product (**a**) as well as the median (**b**) and 25th (**c**), 75th (**d**), 1st (**e**), and 99th (**f**) percentiles of the daily sea surface temperature biases between AdriSC ROMS 3 km model results and the AVHRR product during the 1987–2017 period.
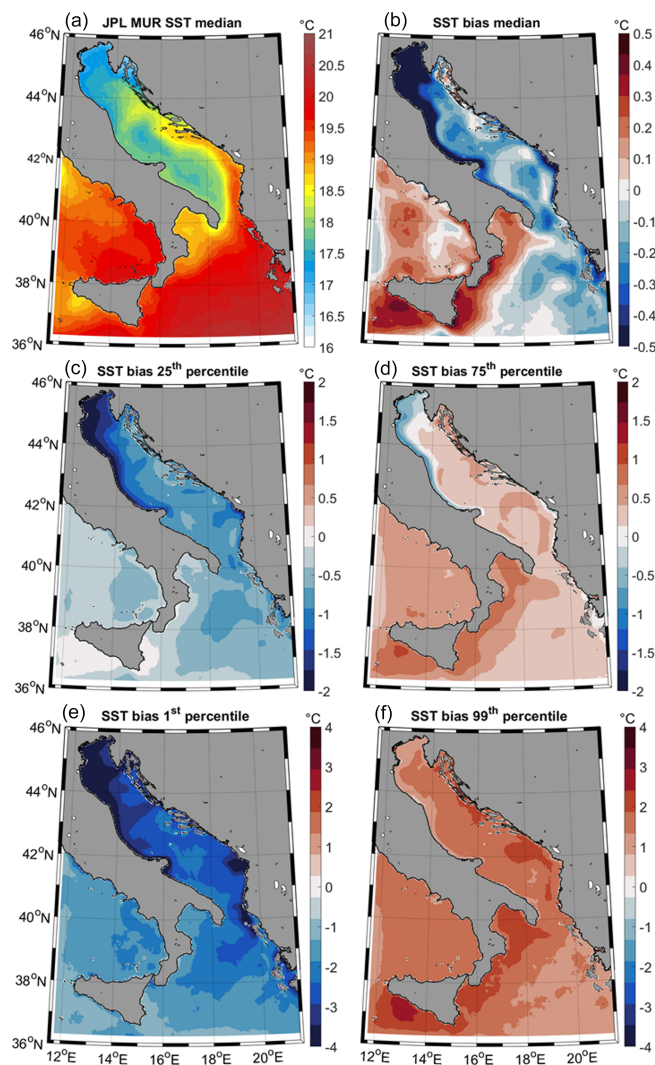
Figure 5. As in Fig. 4 but for the JPL MUR daily sea surface temperature product during the 2002–2017 period.

the Adriatic have surface temperatures around 17.7 °C. The highest temperatures are in the middle and southeastern Adriatic, ranging from 18.5 to 19.5 °C. In the northern Ionian Sea, median temperatures are mostly around 20.0 °C. Concerning the evaluation, the AdriSC ROMS 3 km model generally underestimates the SST, except in the coastal northeastern Adriatic and western part of the Ionian Sea. In the northern Adriatic, northern part of the western coast along the plume of the Po river, and southernmost part of the eastern coast, negative biases reach below −0.5 °C, while in the rest of the Adriatic as well as the middle and eastern parts of the Ionian Sea biases reach down to −0.3 °C. A narrow strip of negative median biases may be seen along the eastern coast of the southern Adriatic, matching the plumes of the

large Albanian rivers. In terms of the extreme conditions, for the 25th percentile, negative biases reach down to −2.0 °C in the northern Adriatic and northern part of the western coast, −1.0 °C in the rest of the Adriatic, and −0.8 °C in the Ionian Sea. For the 1st percentile, biases reach down to −4.0 °C in the northern Adriatic, northern part of the western coast, and southernmost part of the eastern coast, −3.0 to −2.0 °C in the rest of the Adriatic, and −3.0 °C in the Ionian Sea. For the 75th percentile, small negative biases are present in the northern Adriatic and northern part of the western coast down to −0.5 °C, whereas for the rest of the Adriatic and Ionian Sea the temperature is overestimated by up to 0.3–0.8 °C. For the 99th percentile, the model overestimates the SST in the whole domain by up to 0.5–2.0 °C.

3.1.2 Discussion

This brief evaluation of the AdriSC ROMS 3 km sea surface properties thus reveals that the model is capable of reproducing the BiOS, even though with a weaker intensity due to the overestimation of both seasonal and interannual signals. The SST is also quite well reproduced despite presenting a persistent cold bias within the Adriatic Sea.

Within the Mediterranean climate community, the overall cold SST bias, which is present particularly during summer, is a well-known feature of the ocean models. First, following Akhtar et al. (2018) – which assessed the impact of model resolution and coupling in the Mediterranean Sea – coupled atmosphere–ocean models are more likely to generate negative SST biases. Second, a comparison of SST results from six different models with remote sensing products (Darmaraki et al., 2019) has shown cold biases ranging from about -0.3 to $-1.0\,°C$ on average over the entire Mediterranean Sea. Finally, the cold summer SST biases are also known to be higher in the northern Adriatic Sea, reaching below $-3\,°C$ on average (e.g. L'Hévéder et al., 2013; Di Luca et al., 2014; Sevault et al., 2014; Parras-Berrocal et al., 2020). Consequently, it can be safely said that the results obtained with the AdriSC ROMS 3 km model are at least within the ranges of the known cold SST biases of the Mediterranean models. But, following these first results, the high-resolution AdriSC models also seem to improve the representation of the summer SST as the 25th percentile – which is most likely representative of the summer month biases – only reaches a maximum value of $-2\,°C$ near the Po river and is $-0.75\,°C$ on average over the entire Adriatic Sea.

As explained in Parras-Berrocal et al. (2020), the cold summer SST biases of the AdriSC ROMS 3 km model can result from (1) a deficit of solar radiation by the AdriSC atmospheric model, which has shown a systematic temperature underestimation (up to $5\,°C$) during the summer (Denamiel et al., 2021b), (2) some intrinsic shortcomings of the AdriSC ocean model such as vertical mixing and turbidity, and (3) the fact that the river temperatures are imposed by taking the ERA-Interim skin temperatures closest to the river estuaries, which is a crude approximation, particularly for the largest Adriatic rivers such as the Po or the Albanian rivers. Finally, it is known that the optical properties of the water play a crucial role in modelling the turbidity, which is responsible for most of the downward shortwave radiation absorption in the upper layer and thus potentially the presence of cold SST biases. The evaluation of the AdriSC ROMS 3 km SST results may thus also show the limitations of the implemented $\mathrm{d}Q/\mathrm{d}SST$ procedure, which was supposed to mitigate the problems linked to the optical properties of the Adriatic waters.

3.2 Modelled thermohaline properties

3.2.1 Evaluation

The overall skills of the AdriSC ROMS 3 km and 1 km models to reproduce the observed CTD data are presented in Fig. 6.

First, correlations and normalized standardized deviations of modelled and observed temperature (Fig. 6a) and salinity (Fig. 6b) for each observational experiment and/or cruise are shown with Taylor diagrams. It should be noticed that the CSP01 dataset presents extremely small correlations for the temperature (0.0 and 0.3 for the AdriSC ROMS 3 km and 1 km models, respectively) and even anticorrelations for the salinity (-0.2 and -0.4 for the AdriSC ROMS 3 km and 1 km, respectively), which are marked as 0.0 on the Taylor diagram for practical reasons. Additionally, for the AdriSC ROMS 1 km model, the CSP01 dataset also presents large standardized deviations for both temperature and salinity (3.9 and 3.7, respectively), which are conveniently marked as 2.0 on the Taylor diagram. Since all the other datasets have relatively similar results, it is suspected that CSP01 may not be a reliable dataset for this evaluation, and it is treated as an outlier and removed from further analysis. For all the other observational experiments and/or cruises, the overall results (hereafter referred to as all data) basically highlight the fact that the AdriSC ROMS 3 km and 1 km models reproduced the observed temperatures with good accuracy (i.e. correlations around 0.9 and normalized standardized deviations around 1.0) but do not properly capture the observed salinity (i.e. correlations around 0.7 and normalized standardized deviations between 0.3 and 0.5). This most probably highlights the fact that even kilometre-scale ocean models struggle to accurately reproduce the freshwater input from the Adriatic rivers, which play a crucial role in terms of the thermohaline circulation along the coasts (Vilibić et al., 2016, 2018). Second, the Q–Q plots of temperature and salinity (Fig. 6c and d) reveal that both models are capable of overall representing the observed distributions with only a small underestimation of the observed temperatures above $22\,°C$ but a substantial overestimation of the observed salinity below 37.5. However, it should be noted that the number of records with salinity lower than 37.5 only represents less than $1\,\%$ of the entire dataset. Additionally, the AdriSC ROMS 1 km model presents significantly smaller salinity overestimations than the AdriSC ROMS 3 km model and is therefore solely used for further evaluation of the modelled thermohaline properties. Finally, the scatter plots (Fig. 6e and f) reveal that the hexagons with the largest number of points follow the reference line for both temperature and salinity, which indicates that the vast majority of the AdriSC ROMS 1 km results correspond well to the observations in both intensity and timing.

A more detailed evaluation of the AdriSC ROMS 1 km thermohaline properties depending on four depth ranges (i.e. 0–50, 50–200, 200–500, and 500–2000 m) is presented as the
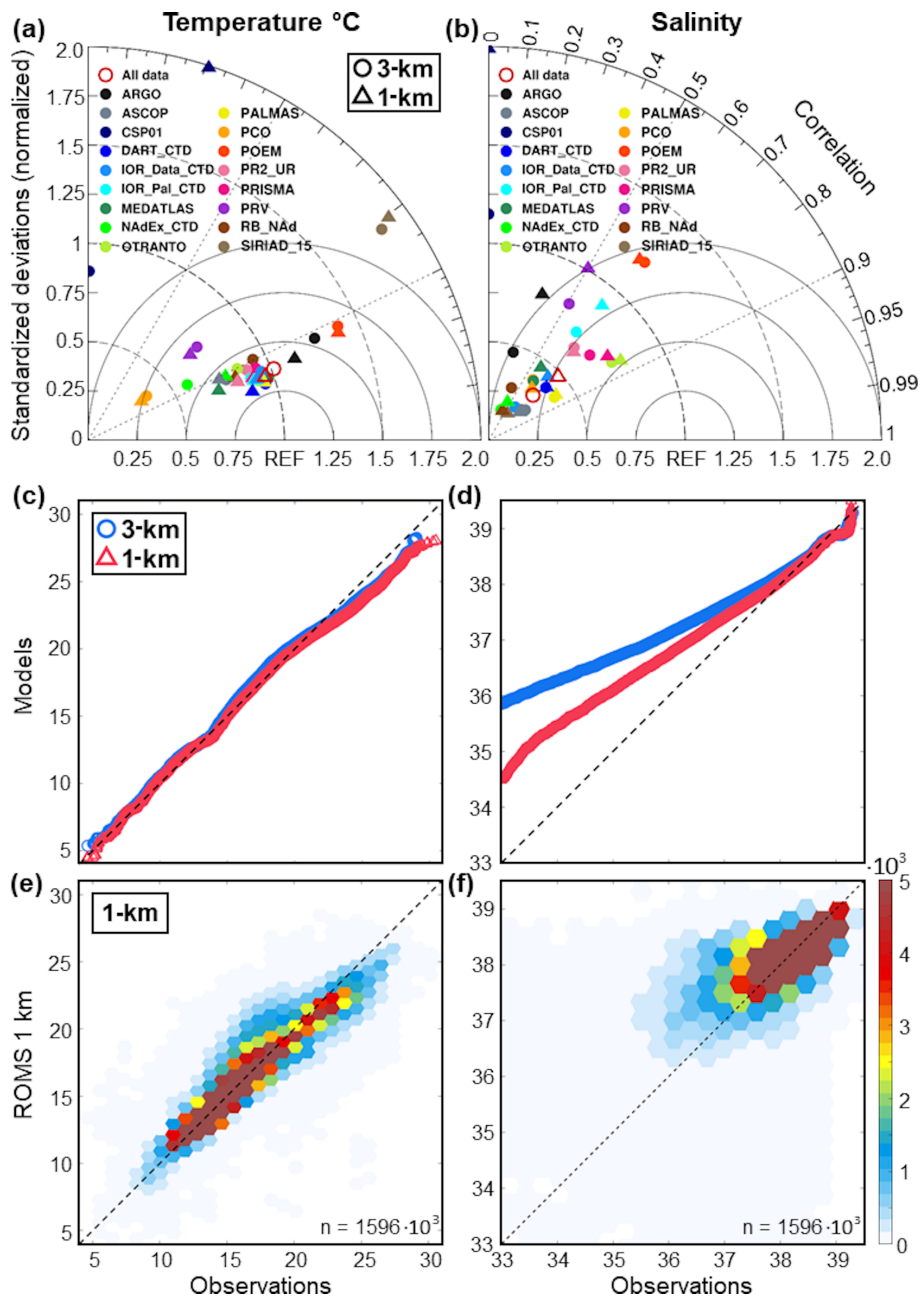
Figure 6. Evaluation of the AdriSC ROMS 3 km and 1 km temperature **(a, c, e)** and salinity **(b, d, f)** results against observations from 17 different datasets with **(a, b)** Taylor diagrams and **(c, d)** quantile–quantile plots as well as, only for the 1 km model, **(e, f)** scatter plots showing the density (number of occurrences) with hexagonal bins and total number of points n.

median (Fig. 7) and MAD (Supplement, Fig. S1) of the temperature and salinity biases (i.e. model minus observations), depending on the locations of the in situ observations. For the surface layer (0–50 m), the median temperature and salinity biases (Fig. 7a and b) present a large spatial variability. In general, a slight prevalence of temperature underestimation and salinity overestimation in the whole Adriatic can be noticed. Furthermore, biases are most pronounced in the northern Adriatic, with dominant negative values for temper-

ature ranging from -4 ± 0–0.9 to -2 ± 0–0.9 °C and dominant positive values for salinity up to 4.3 ± 0–1.4. The large overestimation of the salinity in the northern Adriatic upper layer is most probably influenced by the inaccurate representation of the river discharges in the model, especially of the Po river, with the largest outflow in the Adriatic Sea (average discharge of $1500 \, \text{m}^3 \, \text{s}^1$; Raicich, 1996; Supić and Orlić, 1999). Strong negative temperature biases are also present in the middle Adriatic ranging from -2.4 ± 0–0.4 to -0.5 ± 0–

0.4 °C. Furthermore, larger median temperature and salinity biases are present in the northeastern Adriatic coastal areas, particularly in the Kvarner Bay, ranging from -2.0 ± 0.0–1.2 to 1.3 ± 0.0–1.2 °C and -0.7 ± 0.0–1.0 to 2.9 ± 0.0–1.0, respectively. Biases in the western coastal part of the Adriatic range from -1.0 ± 0.0–0.3 to 1.5 ± 0.0–0.3 °C for the temperature and -0.8 ± 0.0–0.2 to 1.5 ± 0.0–0.2 for the salinity. In the middle eastern (including the Dalmatian Islands) and the southern Adriatic, biases are of the order of -1.8 ± 0.0–0.9 to 0.8 ± 0.0–0.9 °C for the temperature and -0.9 ± 0.0–1.0 to 1.7 ± 0.0–1.0 (only -0.4 ± 0.0 to 0.3 ± 0.0 in the southern Adriatic) for the salinity.

For the upper intermediate layer (50–200 m), the model reproduces dominantly warmer temperatures, except in the southern Adriatic where the biases range between -0.7 ± 0.0–0.2 and 0.4 ± 0.0–0.2 °C (Fig. 7c). The largest temperature overestimations are located in the northeastern Adriatic, with biases up to 3.0 ± 0.8 °C, as well as in the middle Adriatic and the middle eastern coastal areas, with biases up to 1.5 ± 0.8 °C. Concerning the salinity, the model generally underestimates the observations (Fig. 7d) except in the northeastern Adriatic where positive salinity biases up to 0.5 ± 0–0.1 are dominant.

For the lower intermediate layer (200–500 m), positive temperature biases up to 1.5 ± 0.0–0.2 °C adjacent to negative biases down to -1.0 ± 0.0–0.2 °C are located in the middle Adriatic and more precisely in the Jabuka Pit, the collector of the northern Adriatic dense waters (Vilibić and Supić, 2005), while negative biases down to -0.8 ± 0.01–0.2 °C are present in the southern Adriatic (Fig. 7e). Salinity biases are slightly negative with values down to -0.1 ± 0.0 (Fig. 7f). For the deeper layers (500–2000 m), temperature is underestimated in the southern Adriatic Pit and in the northern Ionian Sea with biases ranging from -0.1 ± 0.1 to -0.8 ± 0.1 °C (Fig. 7g). Similarly, salinity biases are relatively low and range from -0.1 ± 0.0 to 0.0 ± 0.0 (Fig. 7h). Overall, the spatial analysis of the CTD stations depending on the depth reveals that the capability of the AdriSC ROMS 1 km model to reproduce temperature and salinity is generally better in deeper parts of the Adriatic than in the coastal areas and the shallow northern Adriatic shelf.

The last kind of analysis is an in-depth climatological and seasonal evaluation of the AdriSC ROMS 1 km thermohaline properties performed for seven predefined subdomains (Fig. 1b). However, to keep a reasonable article length, only three of these subdomains are fully analysed hereafter (Figs. 8 to 10). For the remaining four subdomains, only a summary is presented, and the full description is provided in the Supplement (Figs. S2 to S5).

For the northern Adriatic subdomain (Fig. 8), the AdriSC ROMS 1 km model is overall lacking accuracy in reproducing the thermohaline properties. The monthly temperature climatology is reproduced relatively well most of the year (i.e. biases ranging from -0.6 ± 1.8 to 0.6 ± 0.3 °C) except in August, September, and October when the differences can
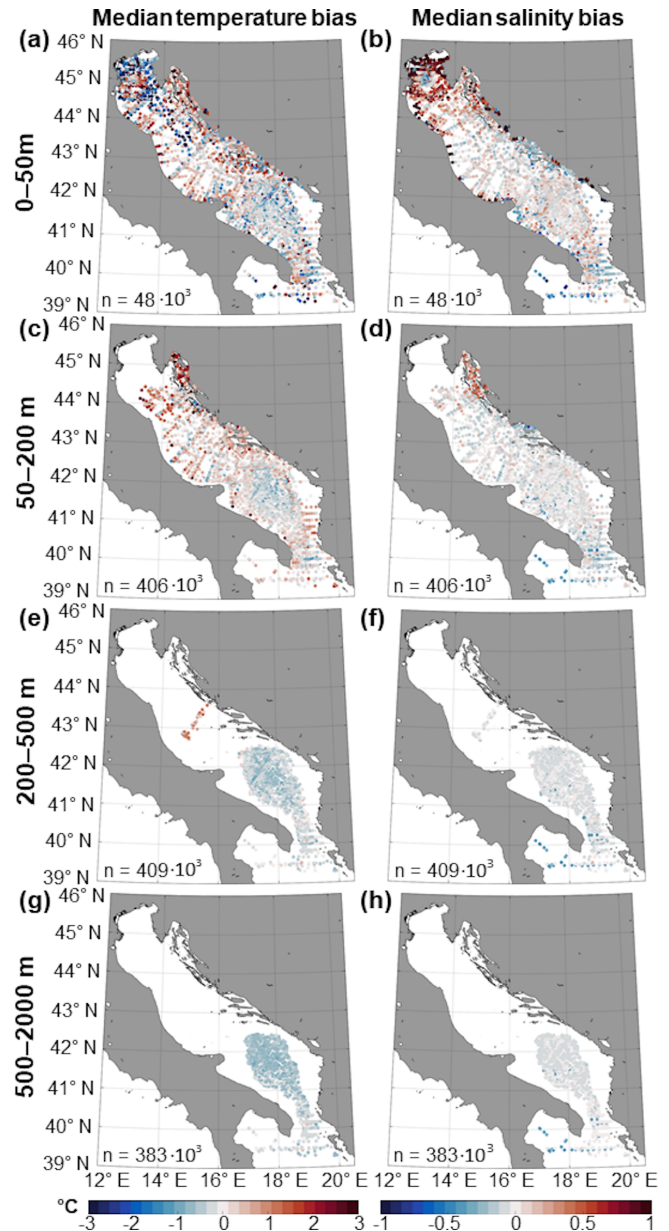

Figure 7. Median of the temperature (left panels) and salinity (right panels) biases between AdriSC ROMS 1 km model results and CTD observations for depth ranges **(a, b)** 0–50 m, **(c, d)** 50–200 m, **(e, f)** 200–500 m, and **(g, h)** 500–2000 m, with the total number of points n (bottom left corner).

reach down to -1.6 ± 1.3 °C (Fig. 8a). The salinity is not well represented, especially in the second half of the year, with persistently higher values by up to 0.7 ± 0.3 (Fig. 8b). Regarding the seasonal variations, the vertical profiles of the median temperature biases show a strong underestimation reaching down to -1.0 °C in spring and -2.0 °C in summer in the surface layer (Fig. 8d). However, during these two seasons, a large overestimation of the temperature is present below 10 m and up to 3.8 °C at 30 m of depth. In autumn,
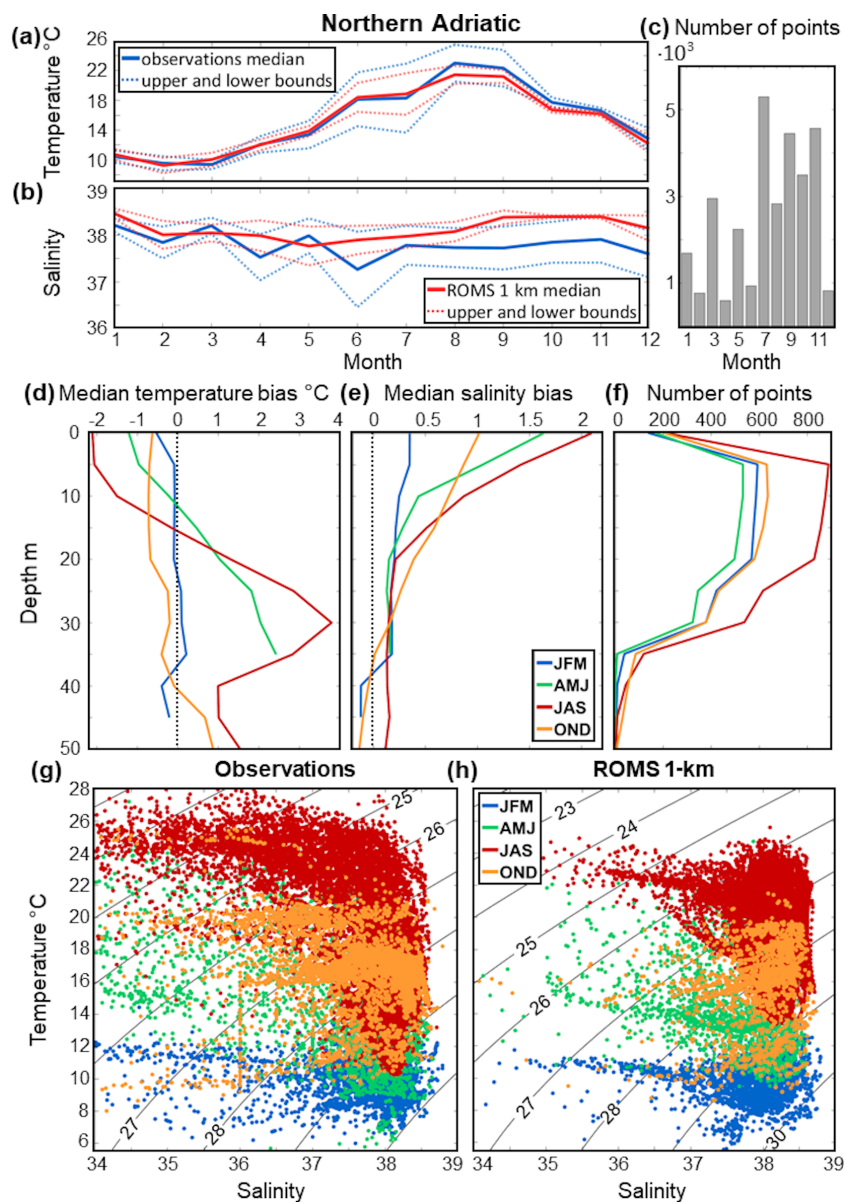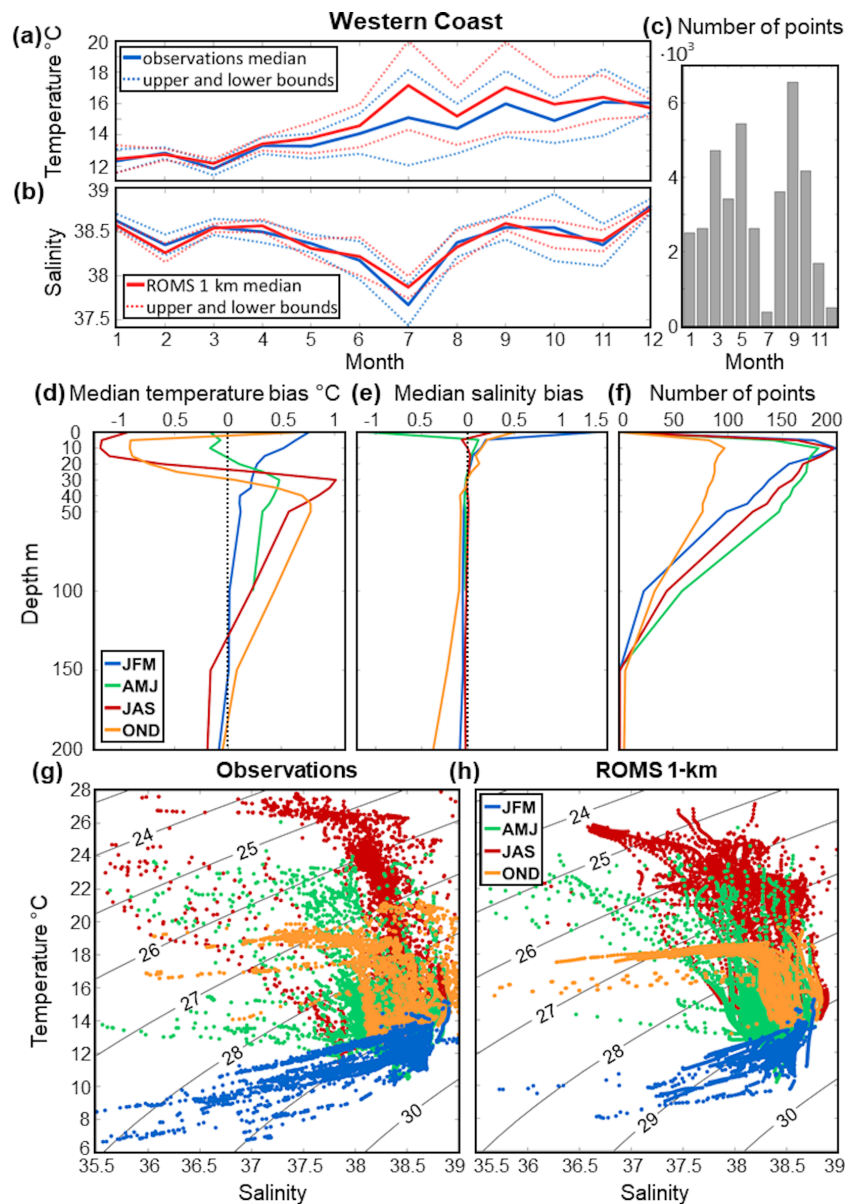
Figure 8. Northern Adriatic subdomain. Monthly climatology of AdriSC 1 km and in situ **(a)** median temperature, **(b)** median salinity, and their variabilities (i.e. upper and lower bounds defined as ±MAD) as well as **(c)** the number of observations per month. Seasonal variations of the **(d)** temperature and **(e)** salinity biases between the AdriSC ROMS 1 km model and observations depending on the depth as well as **(f)** the number of observations per depth. Seasonal $T–S$ diagrams for **(g)** the CTD observations and **(h)** the AdriSC ROMS 1 km model with potential density anomaly (PDA) isolines.

temperature is mostly negatively biased, and the underestimation reaches down to $-0.7\,°C$. Winter temperature biases are rather small throughout the whole water column. In addition, salinity is strongly overestimated at the surface independently of the season (Fig. 8e), with winter having the smallest biases (below 0.5) and summer having the largest biases (up to 2.1). Below 20 m the salinity biases are smaller and the seasonal variability is weaker. The analysis of the $T–S$ diagrams reveals that the model performs well in reproducing dense water masses, and since the northern Adriatic is

well known and one of the most researched dense water formation sites (Zore-Armanda, 1963; Vilibić and Supić, 2005; Mihanović et al., 2013, 2018; Vilibić et al., 2016), these results are promising. The model seems to be less accurate in the density ranges below $25\,kg\,m^{-3}$ in which there is an overestimation of density (Fig. 8g, h). In addition, despite the lack of accuracy of the model for salinities under 36 and temperatures over $24\,°C$, most of the observations are well represented in the $T–S$ diagram with the ROMS 1 km model.

Figure 9. Western coast subdomain. Monthly climatology of AdriSC 1 km and in situ **(a)** median temperature, **(b)** median salinity, and their variabilities (i.e. upper and lower bounds defined as ±MAD) as well as **(c)** the number of observations per month. Seasonal variations of the **(d)** temperature and **(e)** salinity biases between the AdriSC ROMS 1 km model and observations depending on the depth as well as **(f)** the number of observations per depth. Seasonal T–S diagrams for **(g)** the CTD observations and **(h)** the AdriSC ROMS 1 km model with PDA isolines.

For the western coast subdomain (Fig. 9), the AdriSC ROMS 1 km model seems to represent the monthly temperature climatology well (Fig. 9a) despite a tendency to higher positive biases from May to November (up to 1.0 ± 0.8 to 2.0 ± 0.2 °C). To be noted is that the highest bias is found in July when the amount of available data is quite small (Fig. 9c). Furthermore, salinity climatology is reproduced with good accuracy throughout the whole year (Fig. 9b). Seasonally, the strongest temperature biases are observed in summer and autumn: (1) mostly negative in the first 20 m

where they reach down to -1.0 °C and (2) becoming positive below 20 m (up to 1.0 °C) until 200 m where they decrease (Fig. 9d). Winter temperature biases are generally small and decrease with depth to reach nearly 0 °C below 100 m. In spring, the temperature biases are negative in the surface but become positive below 20 m down to 100 m, similarly as in the other seasons. Salinity biases seem to be the strongest in the surface with an underestimation of -1.0 in spring and an overestimation up to 1.5 in winter (Fig. 9e). However, a very small number of observations were recorded at

this depth (Fig. 9f). Additionally, salinity biases are small throughout the water column independently of the season. Finally, the seasonal analysis of the T–S diagrams shows that the AdriSC ROMS 1 km model is capable of reproducing the seasonal properties of the western coast subdomain water masses (Fig. 9g, h), where the outflow of freshened waters from the northern Adriatic occurs (Artegiani et al., 1997; Lipizer et al., 2014; Burrage et al., 2009).

For the deep Adriatic subdomain (Fig. 10), the modelled monthly temperature and salinity medians are lower than the observations throughout the whole year. The highest biases occur in winter and spring, reaching almost $-0.7 \pm 0.2\,°C$ for the temperature (Fig. 10a), while the differences in salinity are smaller than -0.1 ± 0.0 (Fig. 10b). Seasonal analysis shows that the temperature biases are mostly negative, down to $-2.0\,°C$ in the surface in summer, and associated with a small number of observations (Fig. 10d), while below 50 m they are mostly smaller than $-0.5\,°C$ (Fig. 10f). More precisely, the underestimation of the observations is minimized between 50 and 300 m of depth for all seasons, except in winter when the biases reach down to $-0.5\,°C$. However, stronger temperature underestimations are present in the deeper layers between 300 and 900 m of depth but rapidly decrease below 900 m of depth. Salinity is overestimated in summer and winter in the surface layer and mostly underestimated for all the other depths and seasons with biases smaller than -0.1 (Fig. 10e). The seasonal analysis of the T–S diagrams shows that the model performs well independently of the season, with slightly narrower temperature and salinity ranges and an overestimation of densities under $26.5\,\mathrm{kg\,m^{-3}}$, particularly in summer (Fig. 10g, h). The densest waters are captured relatively well, which is important as the deep Adriatic subdomain is a well-known dense water formation site (Vilibić and Orlić, 2001, 2002; Manca et al., 2002; Mantziafou and Lascaratos, 2004, 2008).

For the other subdomains (i.e. middle Adriatic, Otranto–Ionian, Kvarner Bay, and Dalmatian Islands; Figs. S2 to S5) a detailed analysis is presented in the Supplement but can be briefly summarized as follows. In the middle Adriatic subdomain monthly climatologies of temperature and salinity are well captured with slightly negative biases. Vertical profiles of temperature and salinity in the middle Adriatic subdomain reveal that the temperature biases are mostly negative in autumn and positive in winter, while the salinity biases are generally negative except in summer at 10 m of depth. In the Kvarner Bay the AdriSC ROMS 1 km model is capable of reproducing the temperature monthly climatology for the entire year except summer. Salinity is captured relatively well with a certain overestimation. Vertical profiles of temperature are best reproduced in autumn when the biases are very small, while for other seasons there is an overestimation. However, salinity is overestimated the entire year in the whole water column with higher biases in the surface layer. Similar results are obtained for the Dalmatian Islands subdomain regarding the temperature monthly climatology, while the salinity is

slightly underestimated. This subdomain has the largest positive temperature biases in summer and the smallest biases in winter and spring, while the largest salinity underestimations occur in summer and autumn. Lastly, for the Otranto–Ionian subdomain, monthly climatologies of temperature and salinity are well captured. Regarding the vertical profiles, the largest variations of temperature biases are present down to 200 m. Below this depth the biases are similar and negative for all the seasons. Salinity biases are largest between 100 and 200 m, while below this layer the biases are very small. Concerning the T–S diagrams, the model performs well for all the subdomains independently of the season with a common overestimation of the densities lower than $26\,\mathrm{kg\,m^{-3}}$.

3.2.2 Discussion

In summary, the evaluation of the AdriSC ROMS 1 km thermohaline properties shows that the model is overall capable of reproducing, with mostly good accuracy, the temperature and salinity in all of the analysed subdomains. In the middle Adriatic, the western coast, and the middle eastern coastal parts of the Adriatic (e.g. Dalmatian Islands subdomain), monthly climatologies are well represented, whereas the largest biases are found in the surface layer (up to 50 m of depth) during summer with a maximum of $\pm 1.0\,°C$ for the temperature and ± 0.2 for the salinity. These are most probably linked to the quoted problems with the optical properties of the Adriatic waters and/or the river discharges. Additionally, in the deepest parts of the southern Adriatic as well as the Strait of Otranto and the northernmost part of the Ionian Sea, biases are persistently negative in the temperature by about $-0.25\,°C$ on average, while the salinity biases are lower than ± 0.1.

However, in some areas at certain depths and depending on the time of the year, the AdriSC ROMS 1 km model lacks accuracy. In general, the largest differences are found in the northern Adriatic, with negative temperature biases in summer (down to $-2.0\,°C$) associated with large positive salinity biases (up to 2.0) in the surface layer. As seen previously for the SST evaluation, the cold bias is probably linked to the improper estimation of the Po river temperature, while the overestimation of the salinity for the lowest values probably comes from the improper estimation of the Po freshwater fluxes. As similar results (i.e. overestimation of surface salinity and overestimation of the summer temperature in surface) are also found in the northeastern coastal part of the Adriatic and a large scatter of the lowest salinity values is present in Fig. 6, the AdriSC ROMS models seem to struggle to reproduce the proper river plume dynamics in the northern Adriatic. Nevertheless, these results still outperform the ones of the previous Mediterranean RCMs evaluated in the Adriatic Sea, which exhibited biases above 3.0 for the salinity and below $-3.0\,°C$ for the temperature in the northern Adriatic (e.g. L'Hévéder et al., 2013; Di Luca et al., 2014; Sevault et al., 2014; Parras-Berrocal et al., 2020). Additionally, indepen-
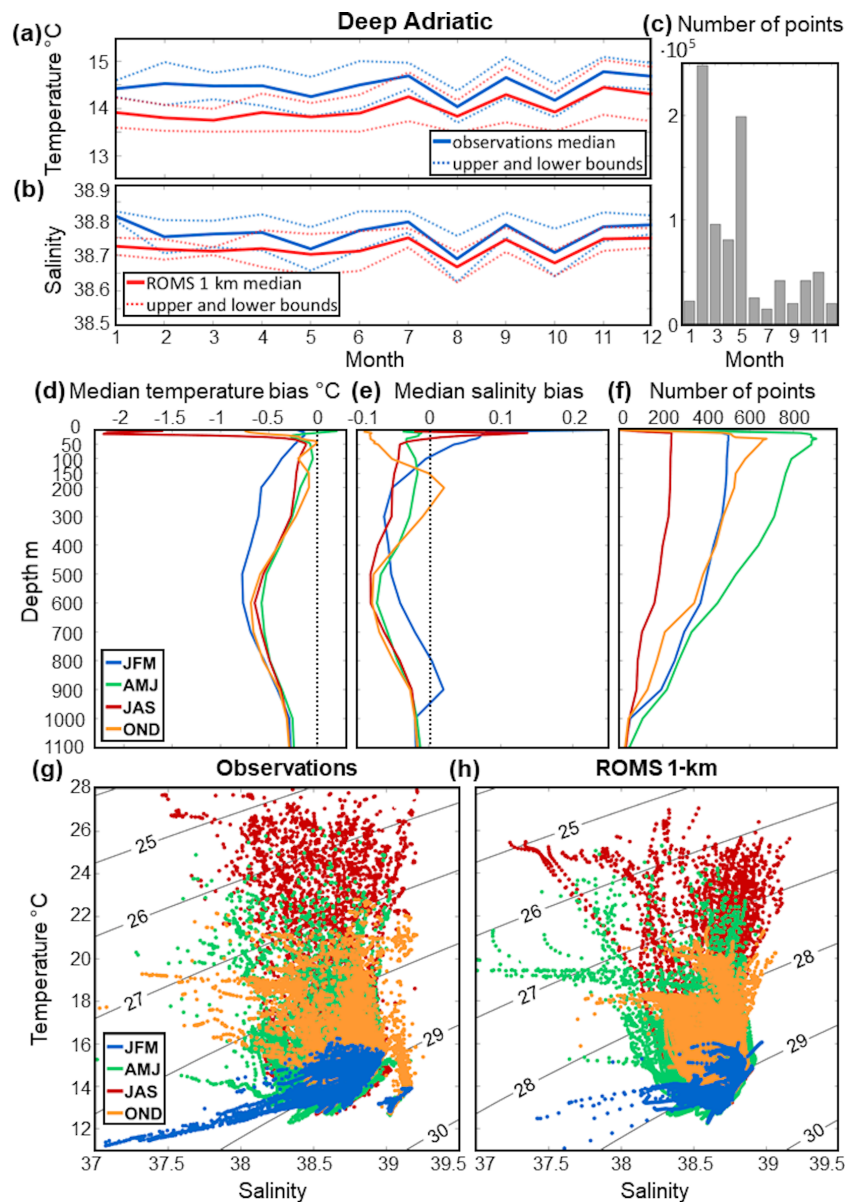
Figure 10. Deep Adriatic subdomain. Monthly climatology of AdriSC 1 km and in situ **(a)** median temperature, **(b)** median salinity, and their variabilities (i.e. upper and lower bounds defined as ±MAD) as well as **(c)** the number of observations per month. Seasonal variations of the **(d)** temperature and **(e)** salinity biases between the AdriSC ROMS 1 km model and observations depending on the depth as well as **(f)** the number of observations per depth. Seasonal $T-S$ diagrams for **(g)** the CTD observations and **(h)** the AdriSC ROMS 1 km model with PDA isolines.

dently of the subdomains, the analysis of the vertical profiles shows that the temperature and salinity biases often present a peak in the vicinity of the thermocline depth, which can probably be linked to an inaccurate representation of vertical diffusivity and vertical mixing in the AdriSC ROMS models. Finally, at the Jabuka Pit, where strong positive temperature biases are adjacent to negative ones, the representation of the bathymetry by the model (e.g. 1 km resolution, flattening due to the smoothing procedure) may have impacted the location and the amount of dense water collected. However, it should

be noted that within the middle Adriatic subdomain, which includes the Jabuka Pit, the coldest more saline waters are well represented by the AdriSC ROMS 1 km model, as seen in the $T-S$ diagram.

Additionally, independently of the subdomains, the analysis of the vertical profiles shows that the temperature and salinity biases often present a peak in the vicinity of the thermocline or halocline depth, which can probably be linked to an inaccurate representation of vertical diffusivity and vertical mixing in the AdriSC ROMS models. However, more

in-depth work should be done to discriminate whether the vertical biases are linked to the AdriSC ROMS model set-up per se or to the MEDSEA fields used as initial and boundary conditions.

3.3 Modelled dynamical properties

3.3.1 Evaluation

A basic skill assessment of the AdriSC ROMS 3 km and one-way nested AdriSC ROMS 1 km models to reproduce the observed ADCP and RCM hourly measurements is presented in Fig. 11.

First, correlations and normalized standardized deviations of the modelled and observed ocean current speeds (Fig. 11a) and directions (Fig. 11b) for each dataset are shown with Taylor diagrams. Following these analyses, the AdriSC ROMS 3 km and 1 km models seem to reproduce the observed correlations between 0.2–0.5 and normalized standardized deviations ranging from 0.5–1.7 for the current speeds as well as correlations around 0.2 and normalized standardized deviations between 0.7–1.1 for the current directions. However, the $Q-Q$ plot analyses of current speeds and directions (Fig. 11c and d) reveal that both models are in fact perfectly capable of representing the observed distributions, except for a small overestimation of the current speeds above $0.5\,\mathrm{m\,s^{-1}}$. Consequently, the low correlations obtained for the Taylor diagrams must have been uniquely linked to a lack of synchronization between hourly observations and model results. It should also be noted that the number of records with speeds higher than $0.5\,\mathrm{m\,s^{-1}}$ represents less than 1 % of the entire dataset. Additionally, the current speed overestimations are smaller for the AdriSC ROMS 1 km results than for those of the AdriSC ROMS 3 km model. Therefore, the AdriSC 1 km model is solely used for further evaluation of the modelled dynamical parameters. Finally, the scatter plot analyses (Fig. 11e and f) show that the hexagons with the highest density of records overall follow the reference line for both current speeds and directions. However, due to the already mentioned lack of synchronization, modelled current speeds, and especially modelled current directions, can be extremely spread out compared to the observations. Despite the inherent difficulties of reproducing the ocean dynamics at the hourly scale, the scattering of the AdriSC ROMS 1 km results can also result from the uncertainties linked to the observational dataset time references. Indeed, due to the lack of metadata availability for a certain number of datasets, some observations, which may have been provided in local time, have been compared with model results in Universal Time Coordinated (UTC). Further, it should be noted that the two vertical lines produced on the current direction scatter plot are in fact inconsistencies identified in the JP2 dataset for two stations and are removed from further analyses.

The last kind of analysis is an in-depth climatological and seasonal evaluation of the AdriSC ROMS 1 km dynamical properties performed for seven different datasets (Fig. 1c). However, to keep a reasonable article length, only three of these datasets are fully analysed hereafter (Figs. 12 to 14). For the remaining four datasets, only a summary is presented, and the full description is provided in the Supplement (Figs. S7 to S10).

For the DART_ADCP dataset (Fig. 12), the monthly climatology differences of the AdriSC ROMS 1 km and the observed current speeds can reach up to $0.02 \pm 0.01\,\mathrm{m\,s^{-1}}$ in October and down to $-0.05 \pm 0.02\,\mathrm{m\,s^{-1}}$ in March (Fig. 12a), while the direction differences reach down to $-39 \pm 48°$ in September. Concerning the seasonal variations, the vertical profiles of the modelled and observed current speeds (Fig. 12d) show an underestimation reaching $-0.03\,\mathrm{m\,s^{-1}}$ in winter and $-0.02\,\mathrm{m\,s^{-1}}$ in spring. The highest differences occur in autumn, reaching down to $-0.05\,\mathrm{m\,s^{-1}}$, while in summer very low biases are present throughout the water column except at 5 m of depth. The rose plots (Fig. 12e) of the modelled and observed current direction reveal that the observed distributions are similarly reproduced by the model independently of the season. It can be seen that the occurrences of the eastward current direction are slightly overestimated, while the northeastward direction is underestimated.

For the JP2 dataset (Fig. 13), AdriSC ROMS 1 km reproduced the monthly climatology of current speed with good accuracy (Fig. 13a), which is supported with a large number of observations throughout the year (Fig. 13c). The largest difference of $0.02 \pm 0.01\,\mathrm{m\,s^{-1}}$ is reached in November. However, the current direction climatology is mostly overestimated, reaching up to $87.43 \pm 7.16°$ in June (Fig. 13b). Seasonal vertical profiles of the modelled and observed current speed (Fig. 13d) show an overestimation under 10 m in winter and autumn, reaching up to $0.03\,\mathrm{m\,s^{-1}}$. Extremely low biases are present in spring and summer down to 40 m of depth below, where they reach $0.02\,\mathrm{m\,s^{-1}}$. According to the rose plots (Fig. 13e), the main current directions within this dataset are well reproduced for all seasons and with a slight overestimation of occurrences of all directions, except the eastward direction, which is strongly underestimated independently of the season. This systematic underestimation may be ascribed to the inaccurate representation of the coastline in the model at the locations of the extracted points.

For the IOR_Data_RCM dataset (Fig. 14), the monthly climatology of current speed in summer and autumn is well represented by AdriSC ROMS 1 km, while the differences are more pronounced in winter and spring, varying between -0.03 ± 0.02 and $0.03 \pm 0.02\,\mathrm{m\,s^{-1}}$ (Fig. 14a). The current direction climatology is reproduced with good accuracy by the model, except in winter when the biases reach up to $50 \pm 29°$ in January (Fig. 14b). Regarding the seasonal variations, the vertical profiles of the modelled speed are generally in good agreement with the observed speed in the first
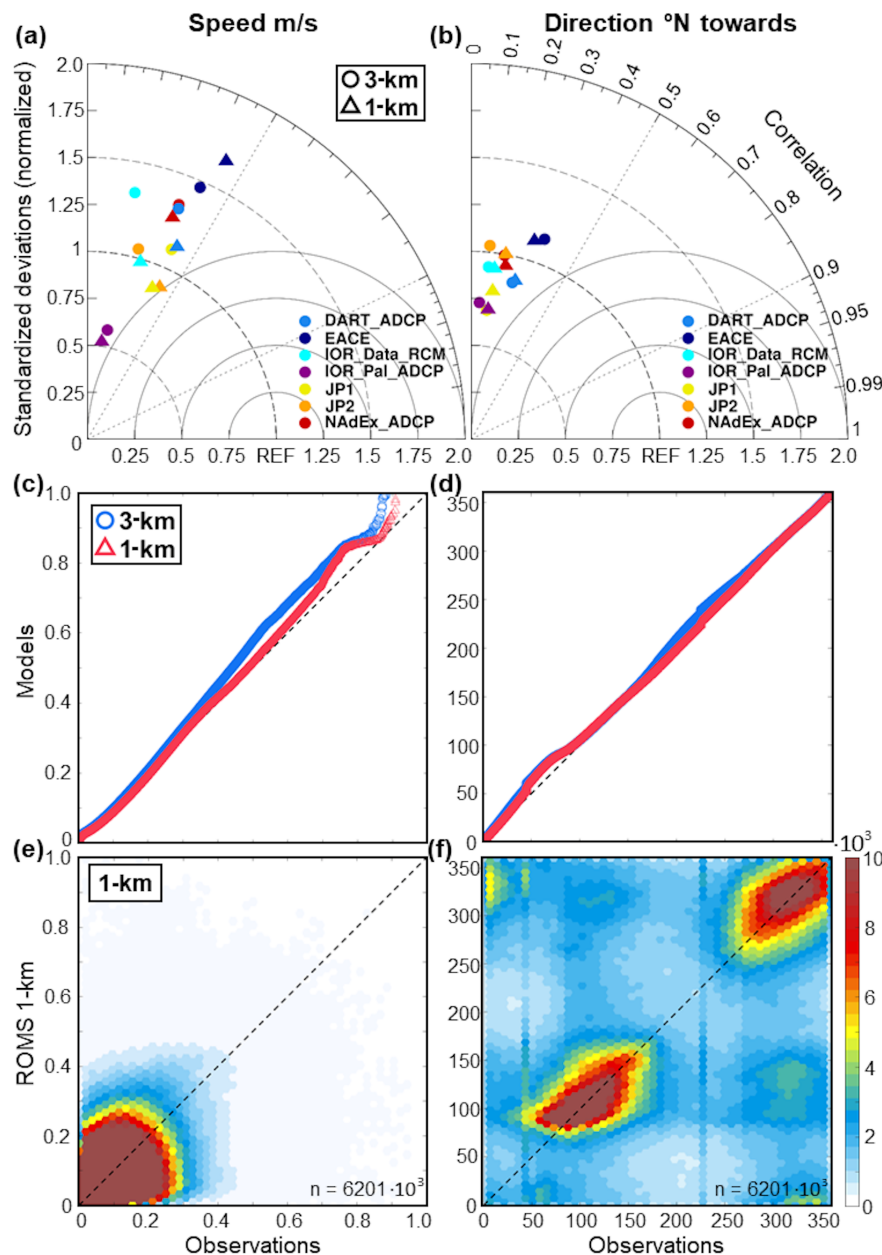
Figure 11. Evaluation of the AdriSC ROMS 3 km and 1 km current speeds **(a, c, e)** and directions **(b, d, f)** against observations from seven different datasets with **(a, b)** Taylor diagrams and **(c, d)** quantile–quantile plots as well as, only for the 1 km model, **(e, f)** scatter plots showing the density (number of occurrences) with hexagonal bins and total number of points n.

40 m (Fig. 14d). Within this layer, very small differences are present in winter and autumn, while in summer and spring the model tends to underestimate the observed speed down to $-0.02\,\mathrm{m\,s^{-1}}$. Below this depth, the observations are underestimated for all seasons. To be noted is that the number of observations is largest in the first 50 m, whereas 99.5 % of all the data is concentrated within the first 100 m. The rest of the data (i.e. 0.5 %) are spread between 100 and 900 m of depth, and thus only the first 100 m are presented on the vertical plots. Lastly, the rose plots of the modelled and observed

current direction (Fig. 14e) reveal that the observed distributions are similarly reproduced by the model independently of the season. The direction differences are slightly larger in autumn for the eastern currents.

For the other datasets (Figs. S6 to S9), monthly climatology and the seasonal vertical profiles of the current speed are mostly underestimated by the AdriSC ROMS 1 km model for the JP1 and IOR_Pal_ADCP dataset. The monthly climatology of the current direction for the JP1 dataset has small positive differences, and the distributions show an overestimation
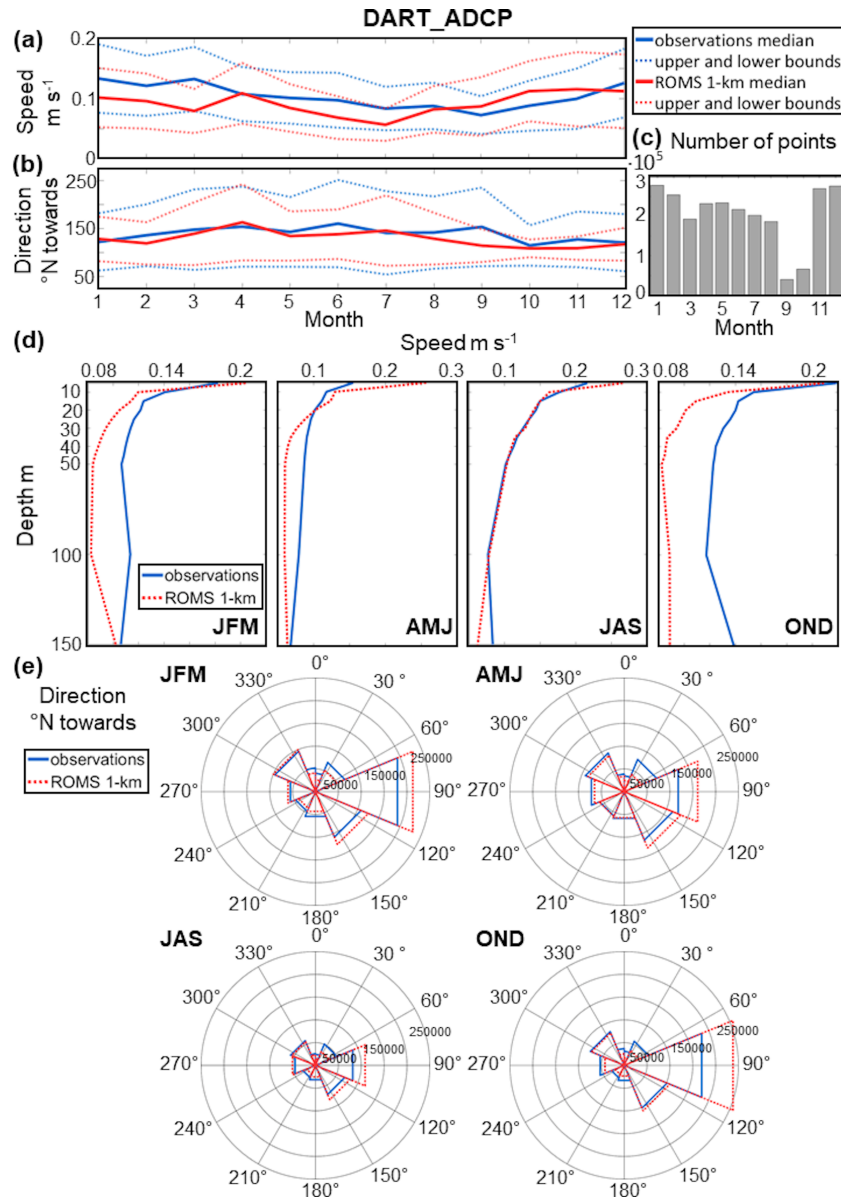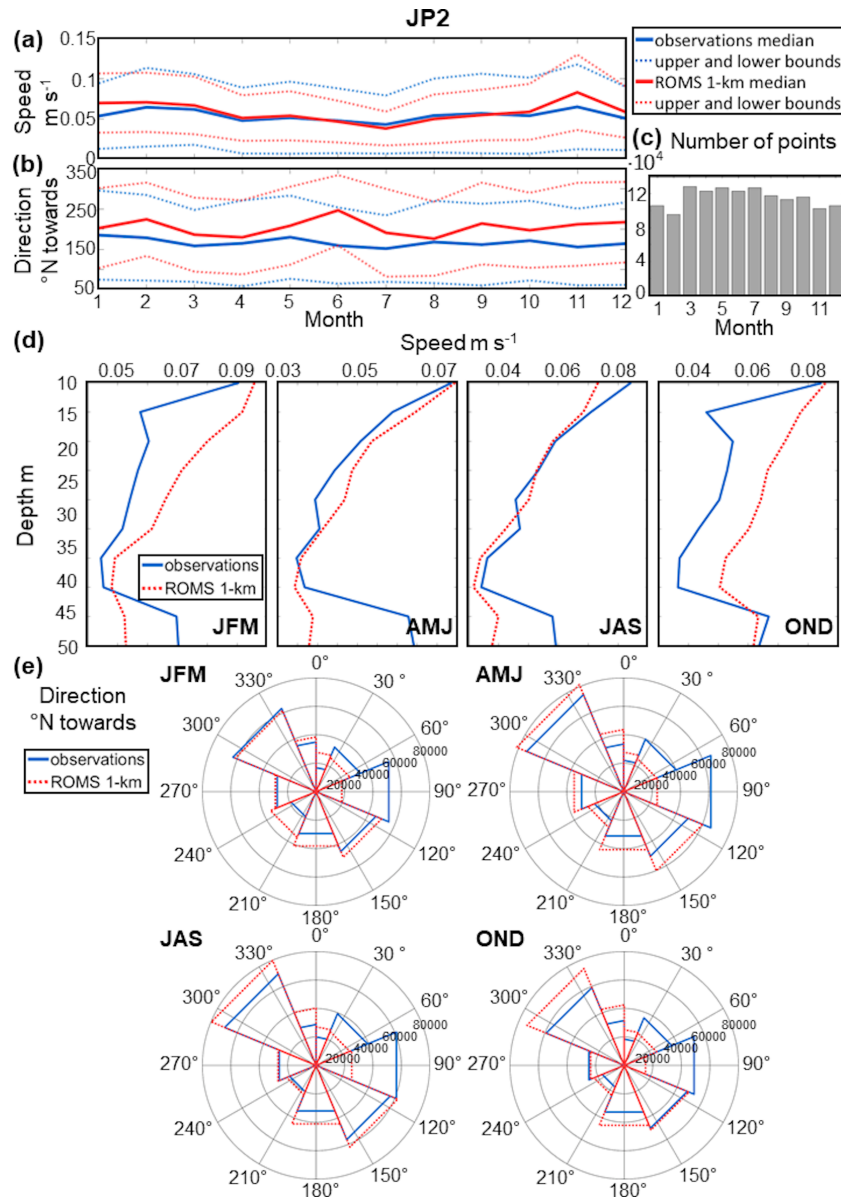
Figure 12. DART_ADCP dataset. Monthly climatology of AdriSC 1 km and in situ **(a)** median speed, **(b)** median direction, and their variabilities (i.e. upper and lower bounds defined as ±MAD) as well as **(c)** the number of observations per month. Seasonal variations of the **(d)** speed of the AdriSC ROMS 1 km model and observations depending on the depth. Seasonal rose plots of the **(e)** direction for ADCP observations and the AdriSC ROMS 1 km model.

of the southeastward and northwestward current directions in summer and autumn. For the IOR_Pal_ADCP dataset, current direction monthly climatology is mostly underestimated independently of the season, while the main eastward and southeastward current directions are overestimated. The current speed climatology and vertical profiles are generally well reproduced for the NAdEx_ADCP dataset, as is the current direction with small differences between the model and observations. Finally, for the EACE dataset, current speed monthly climatology and vertical profiles show an overestimation in winter and underestimation in summer. The cur-

rent direction monthly climatology is largely underestimated in winter, whereas the biases are small in spring and autumn. According to the distributions, this is particularly true for the main northwestward current direction.

3.3.2 Discussion

In summary, the evaluation of the AdriSC ROMS 1 km dynamical properties reveals that the model is overall in good agreement with the observed hourly ocean current speed and direction. In general, there is a certain mismatch in time of
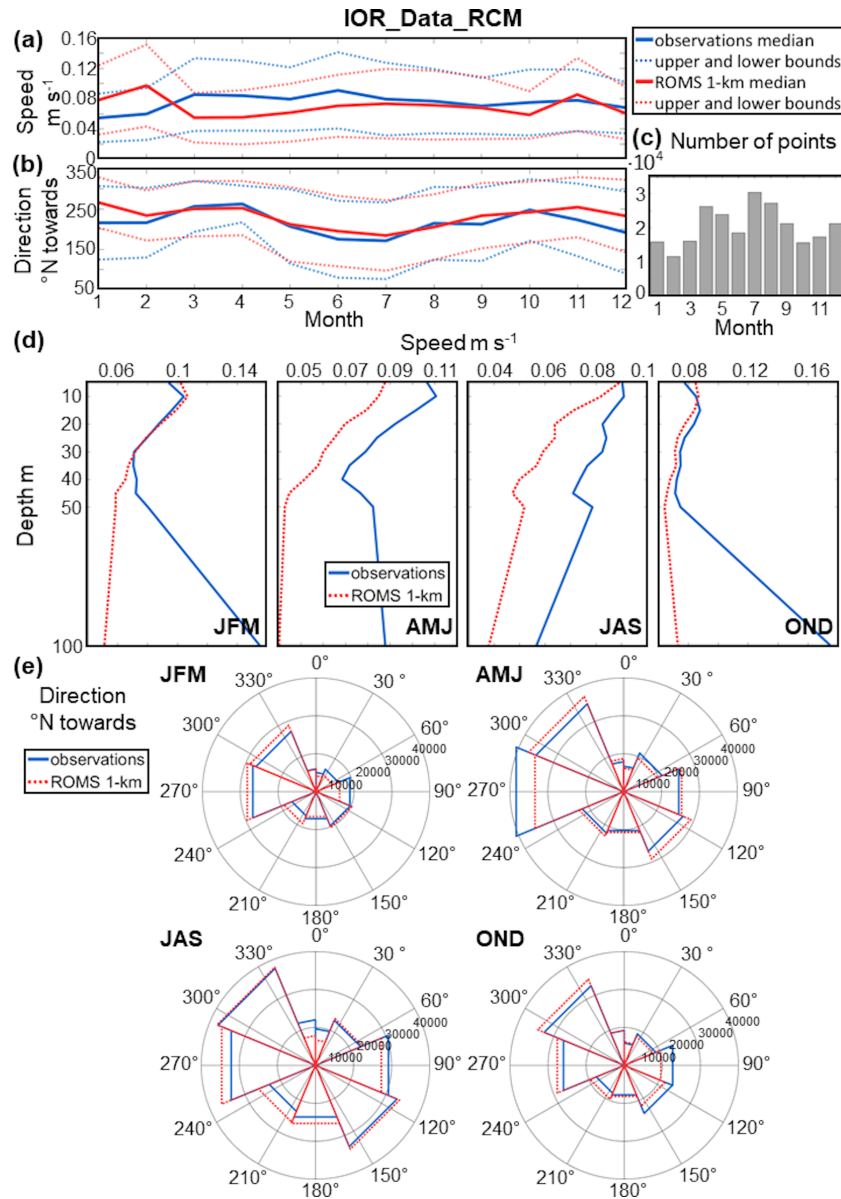
Figure 13. JP2 dataset. Monthly climatology of AdriSC 1 km and in situ **(a)** median speed, **(b)** median direction, and their variabilities (i.e. upper and lower bounds defined as ±MAD) as well as **(c)** the number of observations per month. Seasonal variations of the **(d)** speed of the AdriSC ROMS 1 km model and observations depending on the depth. Seasonal rose plots of the **(e)** direction for ADCP observations and the AdriSC ROMS 1 km model.

the model results and the observations, which may be ascribed to a lack of synchronization between hourly observations and model results as well as to the uncertainties linked to the observational dataset time references. This demonstrates the inherent difficulties of reproducing the ocean dynamics and to evaluate the model results at the hourly scale.

Concerning the datasets, the RCM measurements (i.e. IOR_Data_RCM dataset), which are located mostly along the eastern coast (including islands) and at some offshore locations, are well reproduced by the model with relatively small biases (up to $\pm 0.03\,\mathrm{m\,s^{-1}}$ for the speed and a maximum of 50° for the direction). The ADCP measurements of current speed in the middle eastern coastal area (i.e. JP1 and JP2 datasets) are relatively well captured (biases up to $0.04\,\mathrm{m\,s^{-1}}$), while more significant differences are obtained for the current direction (biases up to 87°). Additionally, a systematic underestimation of the occurrences of the main current directions may be linked to a misrepresentation of the coastline in the model at certain locations. Furthermore, ocean current measurements along the transect across the Palagruža Sill (i.e. DART_ADCP and IOR_Pal_ADCP datasets) are modelled with a general underestimation of cur-

Figure 14. IOR_Data_RCM dataset. Monthly climatology of AdriSC 1 km and in situ **(a)** median speed, **(b)** median direction, and their variabilities (i.e. upper and lower bounds defined as ±MAD) as well as **(c)** the number of observations per month. Seasonal variations of the **(d)** speed of the AdriSC ROMS 1 km model and observations depending on the depth. Seasonal rose plots of the **(e)** direction for RCM observations and the AdriSC ROMS 1 km model.

rent speed (down to $-0.05\,\mathrm{m\,s^{-1}}$) and an overestimation of the occurrences of the main current direction, which can be linked to the bathymetry representation in the model (e.g. 1 km resolution, smoothing procedure). Lastly, the ADCP measurements in the northeastern part of the Adriatic (i.e. NAdEx_ADCP dataset) are reproduced mostly with good accuracy but with a slight underestimation of the current speed (down to $-0.02\,\mathrm{m\,s^{-1}}$). However, a significant improvement is achieved compared to the results of the AL-ADIN/ROMS modelling system, which was evaluated on the same set of measurements from the NAdEx experiment (Vili-

bić et al., 2018). Indeed, the authors have shown that the model strongly underestimated the observed current speeds by 50 %–80 % on average, while AdriSC ROMS 1 km underestimates current speed by only 18 % on average. This highlights the fact that, in the northeastern Adriatic, higher horizontal and vertical ocean and atmospheric model resolutions, better resolving the complex bathymetry and orography, are required to reproduce the mesoscale variability of the winds and particularly the hurricane-strength bora winds, as demonstrated by Denamiel et al. (2021a).

4 Summary and perspectives

In the presented study, the evaluation of the AdriSC ROMS 3 km and one-way nested AdriSC ROMS 1 km ocean models – forced by the already evaluated AdriSC WRF 3 km model (Denamiel et al., 2021b) – has been carried out for a 31-year-long period (1987–2017). The main novelties of the work are, first, the implementation for the very first time – at least to the author's knowledge – of a kilometre-scale one-way coupled atmosphere–ocean model for long-term climate studies, which still presents many challenges (Schär et al., 2020), and, second, the amount of in situ data collected to perform the evaluation of both daily thermohaline (CTD measurements) and hourly dynamical (ADCP and RCM observations) properties of the AdriSC ocean models.

The findings of the evaluation are fourfold. First, the AdriSC ROMS 3 km model has been found to show skill in reproducing (1) the observed decadal signal of sea surface height anomaly interpreted as the BiOS cycles – despite presenting a weaker intensity compared to the seasonal and interannual variabilities – and (2) the observed SST – despite presenting a persistent negative bias within the Adriatic Sea probably linked with the summer cold bias found in the AdriSC WRF 3 km model (Denamiel et al., 2021b). Second, the AdriSC ROMS 1 km model has been found to be more suitable to reproduce the observed daily temperatures and salinities as well as hourly ocean currents than the AdriSC ROMS 3 km model, thus highlighting the necessity for higher-resolution ocean climate simulations in the Adriatic Sea. Then, the detailed analysis of the AdriSC ROMS 1 km simulation revealed that (1) for the daily temperature and salinity, better results are found in the deepest parts than in the shallow shelf and coastal parts, particularly for the surface layer of the Adriatic Sea, while, (2) for the hourly ocean currents, better results are found for the RCMs and ADCPs located along the eastern coast and the northeastern shelf than for the ADCPs located in the middle eastern coastal area and the deepest part of the Adriatic Sea. Finally, the AdriSC ROMS 1 km model was found (1) to perform well in reproducing the seasonal thermohaline properties of the water masses over the entire Adriatic Sea, despite a common overestimation of PDAs lower than 26 kg m^{-3}, and, (2) consequently, to be a suitable modelling framework for studying the long-term thermohaline circulation triggered by the dense waters forming in the northern Adriatic Sea, cascading along the Italian coast, and reaching the northern Ionian Sea where they potentially influence the BiOS regimes. Additionally, it can also be envisioned to study these processes for a far future period (i.e. 2070–2100 period) with the AdriSC long-term projections under climate change scenarios following the pseudo-global warming (PGW; Schär et al., 1996) method. This method has already been tested successfully with the AdriSC model for an ensemble of short-term extreme events in the Adriatic Sea (Denamiel et al., 2020a, b). Therefore, the AdriSC climate simulations are expected

to broaden the knowledge of the dynamics of the Adriatic–Ionian region.

Another important issue raised by this study is that a proper comparison of the ocean climate model skills in the Mediterranean is particularly difficult to achieve due to the absence of standardized ocean observational datasets (similar to the E-OBS products in the atmosphere; https://surfobs.climate.copernicus.eu/dataaccess/access_eobs.php, last access: 20 September 2021). Instead, ocean models are evaluated at different spatial and temporal ranges based on the observational datasets available to given researchers of given countries, which makes a fair comparison between models almost impossible. Therefore, intercomparing ocean climate models in the Mediterranean could only be achieved through the creation of such standardized datasets and, consequently, a change in the ocean data sharing policies, at least at the European level.

Finally, finding the right balance between numerical model accuracy (i.e. resolution) and efficiency (i.e. computational resources and running time) – depending on the temporal and spatial scales of the studied processes – remains one of the major issues of the climate modelling community. For example, (1) the RCMs of the Med-CORDEX community have already been proven to largely underestimate the dense water budget of the Adriatic Sea (Dunić et al., 2019), while (2) the recently developed MEDSEA ocean re-analysis at approximately 4–5 km (Escudier et al., 2020) is forced by the ERA5 atmospheric re-analysis known to underestimate extreme bora events (Denamiel et al., 2021a). To properly capture the Adriatic thermohaline circulation triggered by the dense water formation in the northern Adriatic Sea, the reliability of MEDSEA in the Adriatic Sea thus largely depends on the data assimilation and not the physics. Additionally, even the 1 km resolution used for the AdriSC ocean model is still quite coarse to study the consequences of extreme events along the Adriatic coasts such as flooding in Venice (Denamiel et al., 2020a) or meteotsunamis in Vela Luka (Denamiel et al., 2019). Consequently, it can even be envisioned to downscale the AdriSC climate results during extreme events to a 1.5 km resolution in the atmosphere and up to 10 m (with an unstructured grid) along the coastal areas in the ocean, following the set-up of some operational models in the Adriatic (e.g. for coastal floods; Umgiesser et al., 2021).

In conclusion, the added value of high-resolution coastal models in climate research of complex coastal regions such as the Adriatic has been demonstrated in this study. The main challenges, which include high computational cost and slowness of the models, still remain but may be overcome in the near future due to constant technological and scientific advancements.

Code availability. The code of the COAWST model as well as the ecFlow pre-processing scripts and the input data needed to re-run

the AdriSC climate model in evaluation mode for the 1987–2017 period can be obtained under the Open Science Framework (OSF) FAIR data repository (https://doi.org/10.17605/OSF.IO/ZB3CM, Denamiel, 2021).

References

Akhtar, N., Brauch, J., and Ahrens, B.: Climate modeling over the Mediterranean Sea: impact of resolution and ocean coupling, Clim. Dynam., 51, 933–948, https://doi.org/10.1007/s00382-017-3570-8, 2018.

Amante, C. and Eakins, B. W.: ETOPO1 1 arc-minute global relief model: procedures, data sources and analysis, in: NOAA Technical Memorandum NESDIS, NGDC-24, NOAA, Boulder, Colorado, 2009.

Artegiani, A., Bregant, D., Paschini, E., Pinardi, N., Raicich, F., and Russo, A.: The Adriatic Sea general circulation, part I: air-sea interactions and water mass structure, J. Phys. Oceanogr., 27, 1492–1514, https://doi.org/10.1175/1520-0485(1997)027<1492:TASGCP>2.0.CO;2, 1997.

Batistić, M., Garić, R., and Molinero, J. C.: Interannual variations in Adriatic Sea zooplankton mirror shifts in circulation regimes in the Ionian Sea, Clim. Res., 61, 231–240, https://doi.org/10.3354/cr01248, 2014.

Beg Paklar, G., Isakov, V., Koračin, D., Kourafalou, V., and Orlić, M.: A case study of bora-driven flow and density changes on the Adriatic shelf (January 1987), Cont. Shelf Res., 21, 1751–1783, https://doi.org/10.1016/S0278-4343(01)00029-2, 2001.

Benetazzo, A., Bergamasco, A., Bonaldo, D., Falcieri, F. M., Sclavo, M., Langone, L., and Carniel, S.: Response of the Adriatic Sea to an intense cold air outbreak: Dense water dynamics and wave-induced transport, Prog. Oceanogr., 128, 115–138, https://doi.org/10.1016/j.pocean.2014.08.015, 2014.

Bergamasco, A., Oguz, T., and Malanotte-Rizzoli, P.: Modeling dense water mass formation and winter circulation in the northern and central Adriatic Sea, J. Marine Syst., 20, 279–300, https://doi.org/10.1016/S0924-7963(98)00087-6, 1999.

Boldrin, A., Carniel, S., Giani, M., Marini, M., Bernardi Aubry, F., Campanelli, A., Grilli, F., and Russo, A.: Effects of bora wind on physical and biogeochemical properties of stratified waters in the northern Adriatic, J. Geophys. Res.-Oceans, 114, C08S92, https://doi.org/10.1029/2008JC004837, 2009.

Burrage, D. M., Book, J. W., and Martin, P. J.: Eddies and filaments of the Western Adriatic Current near Cape Gargano: Analysis and prediction, J. Marine Syst., 78, S205–S226, https://doi.org/10.1016/j.jmarsys.2009.01.024, 2009.

Carniel, S., Benetazzo, A., Bonaldo, D., Falcieri, F. M., Miglietta, M. M., Ricchi, A., and Sclavo, M.: Scratching beneath the surface while coupling atmosphere, ocean and waves: Analysis of a dense water formation event, Ocean Model., 101, 101–112, https://doi.org/10.1016/j.ocemod.2016.03.007, 2016.

Cavaleri, L. and Bertotti, L.: In search of the correct wind and wave fields in a minor basin, Mon. Weather Rev., 125, 1964–1975, https://doi.org/10.1175/1520-0493(1997)125<1964:ISOTCW>2.0.CO;2, 1997.

Cavaleri, L., Bertotti, L., Buizza, R., Buzzi, A., Masato, V., Umgiesser, G., and Zampieri, M.: Predictability of extreme meteo-oceanographic events in the Adriatic Sea, Q. J. R. Meteorol. Soc., 136, 400–413, https://doi.org/10.1002/qj.567, 2010.

Cavaleri, L., Abdalla, S., Benetazzo, A., Bertotti, L., Bidlot, J-R, Breivik, Ø., Carniel, S., Jensen, R. E., Portilla-Yandun, Rogers, W. E., Roland, A., Sanchez-Arcilla, A., Smith, J. M., Staneva, J., Toledo, Y., van Vledder, G. P., and van der Westhuysen, A. J.: Wave modelling in coastal and inner seas, Prog. Oceanogr., 167, 164–233, https://doi.org/10.1016/j.pocean.2018.03.010, 2018.

Chapman, D. C.: Numerical treatment of cross-shelf open boundaries in a barotropic coastal ocean model, J. Phys. Oceanogr., 15, 1060–1075, https://doi.org/10.1175/1520-0485(1985)015<1060:NTOCSO>2.0.CO;2, 1985.

Cushman-Roisin, B. and Naimie, C. E.: A 3d finite-element model of the Adriatic tides, J. Mar. Syst., 37, 279–297, https://doi.org/10.1016/S0924-7963(02)00204-X, 2002.

Darmaraki, S., Somot, S., Sevault, F., Nabat, P., Cabos Narvaez, W. D., Cavicchia, L., Djurdjevic, V., Li, L., Sannino, G., and Sein, D. V.: Future evolution of Marine Heatwaves in the Mediterranean Sea, Clim. Dynam., 53, 1371–1392, https://doi.org/10.1007/s00382-019-04661-z, 2019.

Denamiel, C. L.: AdriSC Climate Model: Evaluation Run, OSF [code], https://doi.org/10.17605/OSF.IO/ZB3CM, 2021.

Denamiel, C., Šepić, J., Ivanković, D., and Vilibić, I.: The Adriatic Sea and Coast modelling suite: Evaluation of the meteotsunami forecast component, Ocean Model., 135, 71–93, https://doi.org/10.1016/j.ocemod.2019.02.003, 2019.

Denamiel, C., Pranić, P., Quentin, F., Mihanović, H., and Vilibić, I.: Pseudo-global warming projections of extreme wave storms in complex coastal regions: the case of the Adriatic Sea, Clim. Dynam., 55, 2483–2509, https://doi.org/10.1007/s00382-020-05397-x, 2020a.

Denamiel, C., Tojčić, I., and Vilibić, I.: Far future climate (2060–2100) of the northern Adriatic air–sea heat transfers associated with extreme bora events, Clim. Dynam., 55, 3043–3066, https://doi.org/10.1007/s00382-020-05435-8, 2020b.

Denamiel, C., Tojčić, I., and Vilibić, I.: Balancing accuracy and efficiency of atmospheric models in the northern Adriatic during severe bora events, J. Geophys. Res.-Atmos., 126, e2020JD033516, https://doi.org/10.1029/2020JD033516, 2021a.

Denamiel, C., Pranić, P., Ivanković, D., Tojčić, I., and Vilibić, I.: Performance of the Adriatic Sea and Coast (AdriSC) climate component – a COAWST V3.3-based coupled atmosphere–ocean modelling suite: atmospheric dataset, Geosci. Model Dev., 14, 3995–4017, https://doi.org/10.5194/gmd-14-3995-2021, 2021b.

Di Luca, A., Flaounas, E., Drobinski, P., and Lebeaupin-Brossier, C.: The atmospheric component of the Mediterranean Sea water budget in a WRF multi-physics ensemble and observations, Clim. Dynam., 43, 2349–2375, https://doi.org/10.1007/s00382-014-2058-z, 2014.

Dunić, N., Vilibić, I., Šepić, J., Mihanović, H., Sevault, F., Somot, S., Waldman, R., Nabat, P., Arsouze, T., Pennel, R., Jordà, G., and Precali, R.: Performance of multi-decadal ocean simulations in the Adriatic Sea, Ocean Model., 134, 84–109, https://doi.org/10.1016/j.ocemod.2019.01.006, 2019.

Dutour Sikirić, M., Janeković, I., and Kuzmić, M.: A new approach to bathymetry smoothing in sigma-coordinate ocean models, Ocean Model., 29, 128–136, https://doi.org/10.1016/j.ocemod.2009.03.009, 2009.

Egbert, G. D. and Erofeeva, S. Y.: Efficient inverse modeling of barotropic ocean tides, J. Atmos. Ocean. Technol., 19, 183–204, https://doi.org/10.1175/1520-0426(2002)019<0183:EIMOBO>2.0.CO;2, 2002.

Egbert, G. D., Bennett, A. F., and Foreman, M. G. G.: Topex/Poseidon tides estimated using a global inverse model, J. Geophys. Res., 99, 24821–24852, https://doi.org/10.1029/94JC01894, 1994.

Escudier, R., Clementi, E., Omar, M., Cipollone, A., Pistoia, J., Aydogdu, A., Drudi, M., Grandi, A., Lyubartsev, V., Lecci, R., Cretí, S., Masina, S., Coppini, G., and Pinardi, N.: Mediterranean Sea Physical Reanalysis (CMEMS MED-Currents) (Version 1), Copernicus Monitoring Environment Marine Service (CMEMS) [data set], https://doi.org/10.25423/CMCC/MEDSEA_MULTIYEAR_PHY_006_004_E3R1, 2020.

Flather, R. A.: A tidal model of the north-west European continental shelf, Mem. Soc. R. Sci Liege, 6, 141–164, 1976.

Gačić, M., Civitarese, G., Miserocchi, S., Cardin, V., Crise, A., and Mauri, E.: The open-ocean convection in the Southern Adriatic: A controlling mechanism of the spring phytoplankton bloom, Cont. Shelf Res., 22, 1897–1908, https://doi.org/10.1016/S0278-4343(02)00050-X, 2002.

Gačić, M., Borzelli, G. E., Civitarese, G., Cardin, V., and Yari, S.: Can internal processes sustain reversals of the ocean upper circulation? The Ionian Sea example, Geophys. Res. Lett., 37, L09608, https://doi.org/10.1029/2010GL043216, 2010.

Gačić, M., Civitarese, G., Eusebi Borzelli, G. L., Kovačević, V., Poulain, P.-M., Theocharis, A., Menna, M., Catucci, A., and Zarokanellos, N.: On the relationship between the decadal oscillations of the northern Ionian Sea and the salinity distributions in the eastern Mediterranean, J. Geophys. Res., 116, C12002, https://doi.org/10.1029/2011JC007280, 2011.

Gačić, M., Civitarese, G., Kovačević, V., Ursella, L., Bensi, M., Menna, M., Cardin, V., Poulain, P.-M., Cosoli, S., Notarstefano, G., and Pizzi, C.: Extreme winter 2012 in the Adriatic: an example of climatic effect on the BiOS rhythm, Ocean Sci., 10, 513–522, https://doi.org/10.5194/os-10-513-2014, 2014.

Hersbach, H., de Rosnay, P., Bell, B., Schepers, D., Simmons, A., Soci, C., Abdalla, S., Alonso-Balmaseda, M., Balsamo, G., Bechtold, P., Berrisford, P., Bidlot, J.-R., de Boisséson, E., Bonavita, M., Browne, P., Buizza, R., Dahlgren, P., Dee, D., Dragani, R., Diamantakis, M., Flemming, J., Forbes, R., Geer, A.J., Haiden, T., Hólm, E., Haimberger, L., Hogan, R., Horányi, A., Janiskova, M., Laloyaux, P., Lopez, P., Munoz-Sabater, J., Peubey, C., Radu, R., Richardson, D., Thépaut, J.-N., Vitart, F., Yang, X., Zsótér, E., and Zuo, H.: Operational global reanalysis: Progress, future directions and synergies with NWP, ECMWF ERA Report Series No. 27, https://doi.org/10.21957/tkic6g3wm, 2018.

Horak, J., Hofer, M., Gutmann, E., Gohm, A., and Rotach, M. W.: A process-based evaluation of the Intermediate Complexity Atmospheric Research Model (ICAR) 1.0.1, Geosci. Model Dev., 14, 1657–1680, https://doi.org/10.5194/gmd-14-1657-2021, 2021.

Ivanković, D., Denamiel, C., and Jelavić, D.: Web visualization of data from numerical models and real-time stations network in frame of Adriatic Sea and Coast (AdriSC) Meteotsunami Fore-

cast, OCEANS 2019 – Marseille, France, 17-20 June 2019, 1–5, https://doi.org/10.1109/OCEANSE.2019.8867225, 2019.

Janeković, I. and Kuzmić, M.: Numerical simulation of the Adriatic Sea principal tidal constituents, Ann. Geophys., 23, 3207–3218, https://doi.org/10.5194/angeo-23-3207-2005, 2005.

Janeković, I., Mihanović, H., Vilibić, I., and Tudor, M.: Extreme cooling and dense water formation estimates in open and coastal regions of the Adriatic Sea during the winter of 2012, J. Geophys. Res.-Oceans, 119, 3200–3218, https://doi.org/10.1002/2014JC009865, 2014.

Janeković, I., Mihanović, H., Vilibić, I., Grčić, B., Ivatek-Šahdan, S., Tudor, M., and Djakovac, T.: Multi-platform 4D-Var data assimilation for improving the Adriatic Sea dynamics, Ocean Model., 146, 101538, https://doi.org/10.1016/j.ocemod.2019.101538, 2020.

Johnson, N. C., Krishnamurthy, L., Wittenberg, A. T., Xiang, B., Vecchi, G. A., Kapnick, S. B., and Pascale, S.: The Impact of Sea Surface Temperature Biases on North American Precipitation in a High-Resolution Climate Model, J. Climate, 33, 2427–2447, https://doi.org/10.1175/JCLI-D-19-0417.1, 2020.

JPL MUR MEaSUREs Project: GHRSST Level 4 MUR Global Foundation Sea Surface Temperature Analysis (v4.1), Ver. 4.1. PO.DAAC, CA, USA, https://doi.org/10.5067/GHGMR-4FJ04, 2015.

Krasakopoulou, E., Souvermezoglou, E., Minas, H.J., and Scoullos, M: Organic matter stoichiometry based on oxygen consumption—nutrients regeneration during a stagnation period in Jabuka Pit (middle Adriatic Sea), Cont. Shelf Res., 25, 127–142, https://doi.org/10.1016/j.csr.2004.07.026, 2005.

Larson, J., Jacob, R., and Ong, E.: The model coupling toolkit: a new fortran90 toolkit for building multiphysics parallel coupled models, Int. J. High Perform. Comput. Appl., 19, 277–292, https://doi.org/10.1177/1094342005056115, 2005.

L'Hévéder, B., Li, L., Sevault, F., and Somot, S.: Interannual variability of deep convection in the Northwestern Mediterranean simulated with a coupled AORCM, Clim. Dynam., 41, 937–960, https://doi.org/10.1007/s00382-012-1527-5, 2013.

Ličer, M., Smerkol, P., Fettich, A., Ravdas, M., Papapostolou, A., Mantziafou, A., Strajnar, B., Cedilnik, J., Jeromel, M., Jerman, J., Petan, S., Malačič, V., and Sofianos, S.: Modeling the ocean and atmosphere during an extreme bora event in northern Adriatic using one-way and two-way atmosphere–ocean coupling, Ocean Sci., 12, 71–86, https://doi.org/10.5194/os-12-71-2016, 2016.

Lipizer, M., Partescano, E., Rabitti, A., Giorgetti, A., and Crise, A.: Qualified temperature, salinity and dissolved oxygen climatologies in a changing Adriatic Sea, Ocean Sci., 10, 771–797, https://doi.org/10.5194/os-10-771-2014, 2014.

Liu, F., Mikolajewicz, U., and Six, K. D. : Drivers of the decadal variability of the North Ionian Gyre upper layer circulation during 1910–2010: a regional modelling study, Clim. Dynam., https://doi.org/10.1007/s00382-021-05714-y, 2021.

Ljubenkov, I.: Hydrodynamic modeling of stratified estuary: case study of the Jadro River (Croatia), J. Hydrol. Hydromech., 63, 29–37, https://doi.org/10.1515/johh-2015-0001, 2015.

Ludwig, W., Dumont, E., Meybeck, M., and Heussner, S.: River discharges of water and nutrients to the Mediterranean Sea: major drivers for ecosystem changes during past and future decades?, Prog. Oceanogr., 80, 199–217, https://doi.org/10.1016/j.pocean.2009.02.001, 2009.

Malačič, V. and Petelin, B.: Climatic circulation in the Gulf of Trieste (northern Adriatic), J. Geophys. Res., 114, C07002, https://doi.org/10.1029/2008JC004904, 2009.

Manca, B. B., Kovačević, V., Gačić, M., and Viezzoli, D.: Dense water formation in the Southern Adriatic Sea and spreading into the Ionian Sea in the period 1997–1999, J. Mar. Syst., 33–34, 133–154, https://doi.org/10.1016/S0924-7963(02)00056-8, 2002.

Mantziafou, A. and Lascaratos, A.: An eddy resolving numerical study of the general circulation and deep-water formation in the Adriatic Sea, Deep-Sea Res. I, 51, 251–292, https://doi.org/10.1016/j.dsr.2004.03.006, 2004.

Mantziafou, A. and Lascaratos, A.: Deep-water formation in the Adriatic Sea: interannual simulations for the years 1979–1999, Deep-Sea Res. I, 55, 1403–1427, https://doi.org/10.1016/j.dsr.2008.06.005, 2008.

Marchesiello, P., McWilliams, J. C., and Shchepetkin, A.: Open boundary conditions for long-term integration of regional oceanic models, Ocean Model., 3, 1–20, https://doi.org/10.1016/S1463-5003(00)00013-5, 2001.

Martin, P. J., Book, J. W., Burrage, D. M., Rowley, C. D., and Tudor, M.: Comparison of model-simulated and observed currents in the central Adriatic during DART, J. Geophys. Res., 114, C01S05, https://doi.org/10.1029/2008JC004842, 2009.

May, P. W.: Climatological flux estimates in the Mediterranean Sea: Part 1. Winds and wind stresses, NORDA Report 54, NSTL Station, Mississippi 39529, USA, 1982.

McKiver, W. J., Sannino, G., Braga, F., and Bellafiore, D.: Investigation of model capability in capturing vertical hydrodynamic coastal processes: a case study in the north Adriatic Sea, Ocean Sci., 12, 51–69, https://doi.org/10.5194/os-12-51-2016, 2016.

Mejia, J. F., Koračin, D., and Wilcox, E. M.: Effect of coupled global climate models sea surface temperature biases on simulated climate of the western United States, Int. J. Climatol., 38, 5386–5404, https://doi.org/10.1002/joc.5817, 2018.

Mihanović, H., Vilibić, I., Carniel, S., Tudor, M., Russo, A., Bergamasco, A., Bubić, N., Ljubešić, Z., Viličić, D., Boldrin, A., Malačič, V., Celio, M., Comici, C., and Raicich, F.: Exceptional dense water formation on the Adriatic shelf in the winter of 2012, Ocean Sci., 9, 561–572, https://doi.org/10.5194/os-9-561-2013, 2013.

Mihanović, H., Janeković, I., Vilibić, I., Bensi, M., and Kovačević, V.: Modelling Interannual Changes in Dense Water Formation on the Northern Adriatic Shelf, Pure Appl. Geophys., 175, 4065–4081, https://doi.org/10.1007/s00024-018-1935-5, 2018.

National Centers for Environmental Information: Daily L4 Optimally Interpolated SST (OISST) In situ and AVHRR Analysis, Ver. 2.0. PO.DAAC, CA, USA, https://doi.org/10.5067/GHAAO-4BC02, 2016.

Oddo, P. and Guarnieri, A.: A study of the hydrographic conditions in the Adriatic Sea from numerical modelling and direct observations (2000–2008), Ocean Sci., 7, 549–567, https://doi.org/10.5194/os-7-549-2011, 2011.

Oddo, P., Pinardi, N., and Zavatarelli, M.: A numerical study of the interannual variability of the Adriatic Sea (2000–2002), Sci. Total Environ., 353, 39–56, https://doi.org/10.1016/j.scitotenv.2005.09.061, 2005.

Orlanski, I.: A simple boundary condition for unbounded hyperbolic flows, J. Comput. Phys., 21, 251–269, https://doi.org/10.1016/0021-9991(76)90023-1, 1976.

Orlić, M., Dadić, V., Grbec, B., Leder, N., Marki, A., Matić, F., Mihanović, H., Beg Paklar, G., Pasarić, M., Pasarić, Z., and Vilibić, I.: Wintertime buoyancy forcing, changing seawater properties and two different circulation systems produced in the Adriatic, J. Geophys. Res., 112, C03S07, https://doi.org/10.1029/2005JC003271, 2006.

Pano, N. and Abdyli, B.: Maximum floods and their regionalization on the Albanian hydrographic river network, in: International Conference on Flood Estimation, 6–8 March 2002, CHR. Report II,17, Bern, Switzerland, 379–388, 2002.

Pano, N., Frasheri, A., and Avdyli, B.: The climatic change impact in water potential processe on the Albanian hydrographic river network, in: International Congress on Environmental Modelling and Software, 5–8 July 2010, Ottawa, Ontario, Canada, available at: https://scholarsarchive.byu.edu/iemssconference/2010/all/266 (last access: 20 September 2021), 2010.

Parras-Berrocal, I. M., Vazquez, R., Cabos, W., Sein, D., Mañanes, R., Perez-Sanz, J., and Izquierdo, A.: The climate change signal in the Mediterranean Sea in a regionally coupled atmosphere–ocean model, Ocean Sci., 16, 743–765, https://doi.org/10.5194/os-16-743-2020, 2020.

Pinardi, N., Allen, I., Demirov, E., De Mey, P., Korres, G., Lascaratos, A., Le Traon, P.-Y., Maillard, C., Manzella, G., and Tziavos, C.: The Mediterranean ocean forecasting system: first phase of implementation (1998–2001), Ann. Geophys., 21, 3–20, https://doi.org/10.5194/angeo-21-3-2003, 2003.

Poli, P., Hersbach, H., Dee, D. P., Berrisford, P., Simmons, A. J., Vitart, F., Laloyaux, P., Tan, D. G., Peubey, C., Thépaut, J. N., Trémolet, Y., Hólm, E.V., Bonavita, M., Isaksen, L., and Fisher, M.: ERA-20C: An atmospheric reanalysis of the twentieth century, J. Climate, 29, 4083–4097, https://doi.org/10.1175/JCLI-D-15-0556.1, 2016.

Pranić, P.: Evaluation of the AdriSC Climate Model: Ocean Part, OSF [data set], https://doi.org/10.17605/OSF.IO/W8F4J, 2021.

Prein, A. F., Langhans, W., Fosser, G., Ferrone, A., Ban, N., Goergen, K., Keller, M., Tölle, M., Gutjahr, O., Feser, F., Brisson, E., Kollet, S., Schmidli, J., van Lipzig, N. P. M., and Leung, R.: A review on regional convection-permitting climate modeling: Demonstrations, prospects and challenges, Rev. Geophys., 53, 323–361, https://doi.org/10.1002/2014RG000475, 2015.

Pullen, J., Doyle, J., and Signell, R.: Two-way air–sea coupling: a study of the Adriatic, Mon. Weather Rev., 134, 1465–1483, https://doi.org/10.1175/MWR3137.1, 2006.

Pullen, J., Doyle, J. D., Haack, T., Dorman, C., Signell, R. P., and Lee, C. M.: Bora event variability and the role of air-sea feedback, J. Geophys. Res., 112, C03S18, https://doi.org/10.1029/2006JC003726, 2007.

Raicich, F.: Notes on the flow rates of the Adriatic rivers, Technical Report RF 02/94, CNR, Istituto sperimentale talassografico, Trieste, Italy, 8 pp., 1994.

Raicich, F.: On the fresh water balance of the Adriatic Sea, J. Mar. Syst., 9, 305–319, https://doi.org/10.1016/S0924-7963(96)00042-5, 1996.

Ricchi, A., Miglietta, M. M., Falco, P. P., Benetazzo, A., Bonaldo, D., Bergamasco, A., Sclavo, M., and Carniel, S.: On the use of a coupled ocean–atmosphere–wave model during an extreme cold air outbreak over the Adriatic Sea, Atmos. Res., 172–173, 48–65, https://doi.org/10.1016/j.atmosres.2015.12.023, 2016.

Schär, C., Frei, C., Luthi, D., and Davies, H. C.: Surrogate climate-change scenarios for regional climate models, Geophys. Res. Lett., 23, 669–672, https://doi.org/10.1029/96GL00265, 1996.

Schär, C., Fuhrer, O., Arteaga, A., Ban, N., Charpilloz, C., Di Girolamo, S., Hentgen, L., Hoefler, T., Lapillonne, X., Leutwyler, D., Osterried, K., Panosetti, D., Rüdisühli, S., Schlemmer, L., Schulthess, T. C., Sprenger, M., Ubbiali, S., and Wernli, H.: Kilometer-Scale Climate Models: Prospects and Challenges, B. Am. Meteorol. Soc., 101, E567–E587, https://doi.org/10.1175/BAMS-D-18-0167.1, 2020.

Sevault, F., Somot, S., Alias, A., Dubois, C., Lebeaupin-Brossier, C., Nabat, P., Adloff, F., Déqué, M., and Decharme, B.: A fully coupled Mediterranean regional climate system model: design and evaluation of the ocean component for the 1980–2012 period, Tellus A, 66, 23967, https://doi.org/10.3402/tellusa.v66.23967, 2014.

Shchepetkin, A. F. and McWilliams, J. C.: Correction and commentary for "ocean forecasting in terrain-following coordinates: formulation and skill assessment of the regional ocean modeling system" by Haidvogel et al., J. Comput. Phys., 227, pp. 3595–3624, J. Comput. Phys., 228, 8985–9000, https://doi.org/10.1016/j.jcp.2009.09.002, 2009.

Skamarock, W. C., Klemp, J. B., Dudhia, J., Gill, D. O., Barker, D. M., Wang, W., and Powers, J. G.: A description of the advanced research WRF version 2, NCAR Technical Note, NCAR/TN-468+STR, https://doi.org/10.5065/D6DZ069T, 2005.

Smolarkiewicz, P. K. and Grabowski, W. W.: The multidimensional positive definite advection transport algorithm: nonoscillatory option, J. Comput. Phys., 86, 355–375, https://doi.org/10.1016/0021-9991(90)90105-A, 1990.

Somot, S., Sevault, F., and Déqué, M.: Transient climate change scenario simulation of the Mediterranean Sea for the twenty-first century using a high-resolution ocean circulation model, Clim. Dynam. 27, 851–879, https://doi.org/10.1007/s00382-006-0167-z, 2006.

Somot, S., Ruti, P., Ahrens, B., Coppola, E., Jordà, G., Sannino, G., and Solmon, F.: Editorial for the Med-CORDEX special issue, Clim. Dynam., 51, 771–777, https://doi.org/10.1007/s00382-018-4325-x, 2018.

Supić, N. and Orlić, M.: Seasonal and interannual variability of the northern Adriatic surface fluxes, J. Marine Syst. 20, 205–229, https://doi.org/10.1016/S0924-7963(98)00083-9, 1999.

Taylor, K.: Summarizing multiple aspects of model performance in a single diagram, J. Geophys. Res, 106, 7183–7192, https://doi.org/10.1029/2000JD900719, 2001.

Theocharis, A., Krokos, G., Velaoras, D., and Korres, G.: An internal mechanism driving the alternation of the Eastern Mediterranean dense/deep water sources, in: The Mediterranean Sea: Temporal Variability and Spatial Patterns, Geophysical Monograph Series, edited by: Eusebi Borzelli, G. L., Gačić M., Lionello, P., and Malanotte-Rizzoli, P., AGU, 113–137, https://doi.org/10.1002/9781118847572.ch8, 2014.

Tudor, M., Ivatek-Sahdan, S., Stanešić, A., Horvath, K., and Bajić, A.: Forecasting weather in Croatia using ALADIN numerical weather prediction model, in: Climate Change and Regional/Local Responses, edited by: Zhang, Y. and Ray, P., In-Tech, Rijeka, Croatia, 59–88, 2013.

Umgiesser, G., Bajo, M., Ferrarin, C., Cucco, A., Lionello, P., Zanchettin, D., Papa, A., Tosoni, A., Ferla, M., Coraci, E., Morucci, S., Crosato, F., Bonometto, A., Valentini, A., Orlić, M., Haigh, I. D., Nielsen, J. W., Bertin, X., Fortunato, A. B., Pérez Gómez, B., Alvarez Fanjul, E., Paradis, D., Jourdan, D., Pasquet, A., Mourre, B., Tintoré, J., and Nicholls, R. J.: The prediction of floods in Venice: methods, models and uncertainty (review article), Nat. Hazards Earth Syst. Sci., 21, 2679–2704, https://doi.org/10.5194/nhess-21-2679-2021, 2021.

Umlauf, L. and Burchard, H.: A generic length-scale equation for geophysical turbulence models, J. Mar. Res., 61, 235–265, https://doi.org/10.1357/002224003322005087, 2003.

Vested, H. J., Berg, P., and Uhrenholdt, T.: Dense water formation in the northern Adriatic, J. Mar. Syst., 18, 135–160, https://doi.org/10.1016/S0924-7963(98)00009-8, 1998.

Vilibić, I. and Orlić, M.: Least squares tracer analysis of water masses in the South Adriatic (1967–1990), Deep-Sea Res. I, 48, 2297–2330, https://doi.org/10.1016/S0967-0637(01)00014-0, 2001.

Vilibić, I. and Orlić, M.: Adriatic water masses, their rates of formation and transport through the Otranto Strait, Deep-Sea Res. I, 49, 1321–1340, https://doi.org/10.1016/S0967-0637(02)00028-6, 2002.

Vilibić, I. and Supić, N.: Dense water generation on a shelf: the case of the Adriatic Sea, Ocean Dyn., 55, 403–415, https://doi.org/10.1007/s10236-005-0030-5, 2005.

Vilibić, I., Šepić, and Proust, N.: Observational evidence of a weakening of thermohaline circulation in the Adriatic Sea, Clim. Res., 55, 217–225, https://doi.org/10.3354/cr01128, 2013.

Vilibić, I., Mihanović, H., Janeković, I., and Šepić, J.: Modelling the formation of dense water in the northern Adriatic: sensitivity studies, Ocean Model., 101, 17–29, https://doi.org/10.1016/j.ocemod.2016.03.001, 2016.

Vilibić, I., Mihanović, H., Janeković, I., Denamiel, C., Poulain, P.-M., Orlić, M., Dunić, N., Dadić, V., Pasarić, M., Muslim, S., Gerin, R., Matić, F., Šepić, J., Mauri, E., Kokkini, Z., Tudor, M., Kovač, Ž., and Džoić, T.: Wintertime dynamics in the coastal northeastern Adriatic Sea: the NAdEx 2015 experiment, Ocean Sci., 14, 237–258, https://doi.org/10.5194/os-14-237-2018, 2018.

Vilibić, I., Zemunik, P., Šepić, J., Dunić, N., Marzouk, O., Mihanović, H., Denamiel, C., Precali, R., and Djakovac, T.: Present climate trends and variability in thermohaline properties of the northern Adriatic shelf, Ocean Sci., 15, 1351–1362, https://doi.org/10.5194/os-15-1351-2019, 2019.

Vörösmarty, C., Fakers, B., and Tucker, B.: River discharge database, version 1.0 (RivDIS vLO), volumes 0 through 6, in: A contribution to IHP-V Theme 1, Technical Documents Series, Technical report, UNESCO, Paris, France, 1996.

Warner, J. C., Armstrong, B., He, R., and Zambon, J. B.: Development of a coupled ocean atmosphere-wave-sediment transport (COAWST) modeling system, Ocean Model, 35, 230–244, https://doi.org/10.1016/j.ocemod.2010.07.010, 2010.

Yang, B., Zhang, Y., Qian, Y., Song, F., Leung, L. R., Wu, P., Guo, Z., Lu, Y., and Huang, A.: Better monsoon precipitation in coupled climate models due to bias compensation, npj Clim. Atmos. Sci., 2, 43, https://doi.org/10.1038/s41612-019-0100-x, 2019.

Zavatarelli, M. and Pinardi, N.: The Adriatic Sea modelling system: a nested approach, Ann. Geophys., 21, 345–364, https://doi.org/10.5194/angeo-21-345-2003, 2003.

Zavatarelli, M., Pinardi, N., Kourafalou, V. H., and Maggiore, A.: Diagnostic and prognostic model studies of the Adriatic Sea general circulation: Seasonal variability, J. Geophys. Res., 107, 3004, https://doi.org/10.1029/2000JC000210, 2002.

Zlotnicki, V., Qu, Z., and Willis, J.: SEA_SURFACE_HEIGHT_ALT_GRIDS_L4_2SATS_5DAY_6THDEG_V_JPL1609, Ver. 1812, PO.DAAC [data set], CA, USA, https://doi.org/10.5067/SLREF-CDRV2, 2019.

Zore-Armanda, M.: Les masses d'eau de la mer Adriatique, Acta Adriat., 10, 5–88, 1963.